RESEARCH ARTICLE

VOLCANICA

Q̓welq̓welústen/Mount Meager Volcanic Complex, British Columbia: Inter-eruptive landslide susceptibility assessment using statistical machine learning techniques

Jason P. Connelly*, Sergio A. Sepúlveda, and Glyn Williams-Jones

Centre for Natural Hazards Research, Department of Earth Sciences, Simon Fraser University, Burnaby, B.C., Canada.

Abstract

Over the last 60 years, six landslides with volumes from 10^5 m^3 to 5.3×10^7 m^3 have occurred around Q̓welq̓welústen (Mount Meager Volcanic Complex; MMVC), southwestern British Columbia, Canada. The dormant volcanic massif has experienced significant uplift leading to exposed and incised Miocene and older basement rocks and volcanic rocks associated with the MMVC. The topographic relief and variation in rock types creates a complex environment where the interplay between lithology and landslide initiation can be captured. We developed models using logistic regression and random forest methods to assess the most critical parameters affecting inter-eruptive landslide susceptibility in the area. Both approaches indicate that Devastator Peak and Plinth Peak volcanic assemblages are of notably higher landslide susceptibility. Large landslides originated in higher areas, but long runout poses the main hazard. Results support the need for detailed geological mapping for landslide susceptibility assessments in elevated volcanic massifs worldwide.

Keywords: Inter-eruptive hazards; Deglaciation; Alteration; Uplifted volcanism; Slope stability.

Submitted: 2024-03-21 | Accepted: 2024-06-18 | Published: 2024-09-04

Editor: M. Heap | Typesetter: J. Farquharson

1 Introduction

Volcanoes are complex systems with many factors that can impact landslide susceptibility [van Wyk de Vries and Francis 1997; Voight and Elsworth 1997; van Wyk de Vries and Davies 2015]. A landslide is defined as the movement of a mass of rock, earth or debris down a slope [e.g. Cruden 1991]. Landslide susceptibility is defined as the propensity of an area to failure, and is a function of the stability of the slope and presence of factors which may reduce said stability [Crozier and Glade 2005]. Landslides are commonly classified according to their movement type and the material involved [Hungr et al. 2014] but may be classified according to many other features such as geometry, rate of movement and causes [Varnes 1978]. Landslides may exhibit properties of multiple classes and transition in behaviour [Cruden and Varnes 1996], such as rock slide-debris avalanche, which are typically a result of high entrainment during the failure [Hungr and Evans 2004; Mitchell et al. 2020]. In volcanic terrain, high degrees of heterogeneity can lead to a combination of landslide behaviours simultaneously [Roberti et al. 2017].

Five general methods exist for assigning landslide susceptibility: geomorphological mapping, analysis of landslide inventories, heuristic or index-based approaches, physically based models, and statistically based modelling methods [Guzzetti et al. 1999]. The methods have distinct advantages and disadvantages, which may result in certain methods yielding results that are more accurate, more interpretable, or more transferable to decision-makers, depending on the problem at hand.

The growth of satellite and space-borne data sources has enabled statistically based methods to be completed with greater accuracy, at faster rates and larger scales. Object-oriented image analysis has been applied with a random forest framework to map landslides, identifying several useful features and obtaining good accuracies despite class-imbalance challenges [Stumpf and Kerle 2011]. Similarly, high-resolution LiDAR-derived imagery can be used to extract many useful predictive features for landslides [Chen et al. 2014], as have studies combining multiple spatial data sources [e.g. Zhang et al. 2017]. Accurate and very interpretable results have been obtained with variable selection using penalized regression with high-resolution data [Lombardo and Mai 2018]. Global studies predicting earthquake-induced landslides have achieved good results using a random forest framework and 90-m spatial resolution data [He et al. 2021].

Volcanic sector collapses can produce extremely large-volume landslide events, causing significant risk and altering landscape morphology [Sekiya 1889; Gorshkov 1959; Yonechi 1988; Begét and Kienle 1992; Girina 2013; Shevchenko et al. 2020]. The 1980 Mount St. Helens (USA) eruption provided a wealth of data and knowledge on these processes [Lipman 1981; Moore 1981; Kerr 1984; Siebert and Reid 2023] and recent studies have uncovered entire landscapes formed from these events despite limited evidence from current morphologies. A debris avalanche deposit covering an area greater than 500 km^2 was uncovered at Samalas volcano (Indonesia) using morphological analysis, stratigraphic mapping, and geophysical tools despite no caldera remaining [Malawani et al. 2024]. Based on the extent and sedimentary characteristics of the deposit, it likely formed from a magmatic eruption ~3500 years ago [Malawani et al. 2024]. Determining the origin of volcanic debris avalanche deposits can also be challenging in environments with coalesced volcanic centers and overlapping volcanic periods [Roverato et al. 2018]. Distinguishing between "hot" avalanches produced by processes such as active lava dome collapses and "cold" events occurring as mass wasting events without such conditions is an additional complication;

* jpc19@sfu.ca

however, variations in deposit textures and jointing can be used to distinguish the two [Stewart et al. 2003].

Active volcanoes undergo many volcanic processes and factors linked to increased landslide susceptibility. Among the identified factors are: extensive hydrothermal alteration, magmatic intrusion and extrusion, phreatic and phreatomagmatic explosions, and local ground accelerations from volcanic sources [Voight and Elsworth 1997; Waythomas 2012]. Continental stratovolcanoes typically have weak internal structures due to large pyroclastic rock content and hydrothermal alteration [López and Williams 1993; van Wyk de Vries and Francis 1997; McGuire 2003]. Increases in surface slope, dynamic loading from volcanic earthquakes, and static loading from magma pressure can also affect a slopes susceptibility to failure [Voight and Elsworth 1997]. Low-strength layers such as volcanic residual soils [Hürlimann et al. 2001] or water saturated rock [Siebert 1984] can be additional causes of instability. In the Central Andes, gravitational spreading lead to progressive strain weaking and rock fracturing, as suggested for the Socompa debris avalanche [van Wyk de Vries and Francis 1997; van Wyk de Vries et al. 2001]. Changes in bedrock structure as a result of magmatic intrusion, stress relief, geothermal processes, and destabilization of valley walls can all occur in volcanic environments [Voight and Elsworth 1997], leading to lower rock mass quality. These processes can lead to failures at a range of scales, with smaller events occurring more frequently than large events [McGuire 2003].

Dormant volcanoes which lack recent eruptive activity can still be affected by many of these processes. Small to large landslides can be generated as a result of hydrothermally altered volcanic rocks undergoing preferential gravity-driven spreading [Cecchi et al. 2004] and the associated hazards may be more difficult to predict due to the absence of volcanic precursory signals [Shea and Van Wyk de Vries 2010]. Several recent non-volcanogenic events (i.e. not triggered by an eruption) highlight the importance of mass movement events in these environments. The glaciated dormant Kazbegi stratovolcano, near the Georgia-Russia border, last erupted about 6000 years ago [Chernyshev et al. 2002] and is the site of at least six large ice-rock avalanches, with the largest being a 2002 event of $>1.5 \times 10^8$ m^3 of ice and debris [Evans et al. 2009; Tielidze et al. 2019]. The latest event in 2014 resulted in nine fatalities and damaged critical infrastructure. Causes of significant landslide activity in the area are attributed to unstable glacier dynamics, active displacement of morphostructural blocks, and volcanic activity [Tielidze et al. 2019]. The Yate volcano, a glaciated stratovolcano in the Andean Southern Volcanic Zone of Chile, has no historically recorded eruptions, although tephrochronological evidence suggests minor postglacial explosive activity [Watt et al. 2009]. A detailed study of the 1965 Yate landslide ($6–10 \times 10^6$ m^3) showed that it initiated as a deep-seated rock failure and transformed into a debris flow that flowed down the El Derrumbe valley. An impulse wave generated from the landslide material contacting the Lago Cabrera resulted in the deaths of 27 nearby inhabitants. A fault zone in the complex and late-Pleistocene deglaciation are all factors that may affect volcanic landslide frequency at the site [Watt et al. 2009].

Similar landslide hazards have been identified in the rapidly uplifted mountains surrounding Mount Shirouma in Japan, including rock slope deformation, shallow landslides, toppling and landslide complexes [Kariya et al. 2006]. The area was glaciated during Marine isotope stage 4 (MIS) and MIS 2, and has a complex geological history with Paleozoic to Mesozoic basement rocks and Neogene to Quaternary volcanic rocks. Debris avalanches were found to occur in the study area, but only incorporated volcanic source material with the latest large-volume event in 1911 having an estimated volume of 1.5×10^8 m^3. Many lodges and tourism facilities have been built in the area since the 1970s. Although further study of precursory causes is needed, stress release due to deglaciation, increased precipitation since the early Holocene and permafrost degradation are believed to be the most likely causes [Kariya et al. 2006]. Iliamna volcano, a Quaternary andesitic stratovolcano located in Alaska's Cook Inlet [Werner et al. 2022], also hosts several large glaciers [Waythomas and Miller 1999; Toney et al. 2021] and has undergone rapid uplift and erosion since 15 Ma that exposed plutonic bedrock [Detterman and Hartsock 1966; Vallier et al. 1994]. Although it underwent periods of unrest in 1996, 2002 to 2006, and 2012, no historical eruptions are known to have occurred [Werner et al. 2022]. The massif nevertheless frequently produces large-volume ice-rock avalanches, with at least 8 events $> 5 \times 10^6$ m^3 in the last 65 years and events on the order of 1×10^6 m^3 to 3×10^7 m^3 estimated to occur with return periods of 2–4 years [Huggel et al. 2007]. Low rock strength due to hydrothermal alteration and subsurface heat flow from the volcanic system leading to ice melting at the glacier-rock interface are likely reasons for the occurrence and frequency of events [Huggel et al. 2007; 2008].

In 2010, a large landslide occurred on the flank of Q̓welq̓welústen (Mount Meager) which is a stratovolcano complex in the northern Cascades of British Columbia, Canada. The landslide occurred as multiple events with a total volume of 53×10^6 m^3 [Guthrie et al. 2012; Roberti 2018]. Deposit characteristics indicate the landslide occurred as water-rich and water-poor phases, resulting in different behaviours [Roberti et al. 2017]. The flow from the event travelled 7.8 km downstream from its source location, briefly dammed both Meager Creek and the Lillooet River and forced the temporary evacuation of ~1500 residents in the village of Pemberton. Glacial retreat exposing a zone of extensively hydrothermally altered rock and increased snowmelt due to high temperatures were attributed to the failure [Roberti 2018], with water building up in the fractured volcanic mass [Delcamp et al. 2016].

The Mount Meager Volcanic Complex (MMVC) in southwestern British Columbia (Figure 1), is the most active volcano in Canada with the main syn-eruptive landslide hazards considered to be lahars that may occur in conjunction with dome-collapse pyroclastic density currents and tephra fallout [Hickson et al. 1999; Simpson et al. 2006; Friele et al. 2008; Warwick et al. 2022]. Currently dormant, the glaciated stratovolcano complex has been the site of at least seven very large ($> 1 \times 10^6$ m^3 [Fell 1994]) inter-eruptive landslides in historical time [Friele et al. 2008; Guthrie et al. 2012]. exposing a zone of extensively hydrothermally altered rock. Other stud-

ied events include a large-volume debris flow in July 1998 (1.2×10^6 m^3 [Bovis and Jakob 2000]), a rock avalanche in 1986 (0.5×10^6 m^3 [Evans 1987]), multiple debris flows (10^2 to 10×10^6 m^3 [Jordan 1995]) and a fatal rock avalanche in 1975 (28×10^6 m^3 [Mokievsky-Zubok 1977]). Large-volume pre-historic landslides originating near Q̓welq̓welústen have also been studied [Friele and Clague 2004; Friele et al. 2005] while many other smaller magnitude events frequently occur on the massif but are undocumented in the literature. In addition to studies of individual events, many previous academic and industry assessments of inter-eruptive hazards in the area have been undertaken [e.g. Baumann Engineering 1999; Friele et al. 2008; Friele 2012; Hetherington 2014; Roberti 2018] and provide an invaluable resource for validating results from this study.

An increased landslide occurrence in the volcanic edifice compared to basement areas aligns with previous studies in the region. Holm et al. [2004] studied the occurrence of landslides in relation to post-Little Ice Age neoglacial retreat. Rock falls, rock slides, rock avalanches, debris slides, debris avalanches, and slopes undergoing deep-seated gravitational deformation were mapped northwest of Pemberton, including some in the MMVC. Amongst other findings, the study showed that landslide susceptibility is significantly higher in Quaternary volcanic rocks, such as most of the MMVC, compared to nearby granitic units [Holm et al. 2004].

Rapid uplift in tectonic convergent landscapes leads to the development of elevated headwalls and the steepening of the valley floor section near glaciers as a secondary response [Brocklehurst and Whipple 2007], often resulting in high mean slope angles near the threshold for bedrock landslide initiation [Burbank et al. 1996]. Landslide occurrence is also the dominant mechanism of hillslope erosion in mountainous, tectonically active environments [Hovius et al. 1997; Hewitt 1998; Brocklehurst and Whipple 2007] and allows for equilibrium to be maintained between bedrock uplift and valley incision [Burbank et al. 1996]. Along the British Columbia coast, rapid uplift has also occurred around 12–12.5 ka following ice removal from the Fraser Glaciation [James et al. 2000; Clague and James 2002].

Uplifted basement rocks and volcanic terrain have additional implications for landslide hazards. Both basement rocks and volcanic material are exposed to similar geomorphological processes that may influence slope stability. Additionally, volcanic and basement rock can have varying strength properties that may result in variations in mean slope angles required for landslide initiation. These may have varying effects depending on the slope scale and stress conditions imposed on the material. The purpose of this study is to assess the most important factors controlling landslide occurrence in Q̓welq̓welústen/MMVC (excluding syn-eruptive lahars) using statistically based machine learning techniques. The interaction between basement rocks and volcanic materials in the context of landslide hazards can be readily studied because of the consistent morphological elements affecting both materials. Results have implications to other elevated volcanic massifs around the world, such as the Patagonian Andes, Japan, Alaska, Caucasus, Turkey, New Zealand, the northern Cascades, and Costa Rica, amongst others.

2 Study area

The Mount Meager Volcanic Complex (MMVC) is an active, Pleistocene to Recent glaciated volcanic complex located about 150 km north of Vancouver, British Columbia (Figure 1). The MMVC forms part of the Garibaldi Volcanic Belt, the northern segment of the Cascade Volcanic Arc, and sits within the Coast Mountains, a chain of plutonic intrusions with associated metamorphic pendants and screens [Gehrels et al. 2009]. Eruptions over the past 1.9 Ma from multiple coalesced stratovolcanic centres and spanning compositions from basaltic through to rhyodacite, have generated the current geological setting [e.g. Read 1977; Hickson et al. 1999; Russell et al. 2023; Muhammad et al. 2024]. The volcanic massif is located within the Líl̓wat Nation Traditional Territory, at the headwaters of a populated agricultural valley, and with part of the massif in a provincial park. In addition, a run of river hydroelectric facility, pumice quarries, forestry tenures, and geothermal energy prospects are on or immediately next to the volcano.

The MMVC has also undergone large amounts of uplift [Farley et al. 2001] from the surrounding Coast Mountains due to the subducting Farallon plate (Juan de Fuca, Explorer, and Gorda plates) [Hildreth 2007; Russell et al. 2023] and effects of the Northern Cordilleran slab window [Thorkelson et al. 2011; Russell et al. 2023]. The southern Coast Mountains underwent moderately rapid uplift during the Eocene, followed by very low (~0.02 km Ma^{-1}) uplift rates up to 10 Ma [Parrish 1983]. Steady exhumation of ~0.22 mm yr^{-1} followed, until uplift rates accelerated by at least 70 % post-4 Ma [Farley et al. 2001]. Volcanic stratigraphy of faults in the complex suggests that approximately 1 km of uplift and erosion of volcanics may have been accommodated in the last 5 Ma [Muhammad et al. 2024]. Many large-scale glaciations have occurred in British Columbia over the last several Ma [Souther and Symons 1974; Hickson and Souther 1984] resulting in downwarping and subsequent uplift upon ice removal. Most recently, rapid deglaciation following the Fraser Glaciation triggered rapid land uplift around 12 ka [Mathews et al. 1970; Clague et al. 1982; James et al. 2000; Clague and James 2002]. As a result of uplift, both basement and volcanic rocks have been incised by glaciations [Ryder and Thomson 1986; Jennings et al. 2007], leading to high glacial and glaciofluvial erosion rates [Shuster et al. 2005; Ehlers et al. 2006; Andrews et al. 2012]. This behaviour stands in contrast with volcanic edifices in the southern half of the Cascade Volcanic Arc which have undergone much lesser degrees of uplift [Hammond 1979], including much lower isostatic rebound from deglaciation following the Fraser Glaciation, indicated by elevations of glacial lake shorelines in the northern Cascadia subduction zone [Mathews et al. 1970; James et al. 2000; Clague and James 2002]. Similar uplift histories have occurred at volcanic massifs in the Coast Mountains and northern Cascade Range [Reiners et al. 2002].

Volcanic rocks and nearby basement materials at the complex were first mapped by Read [1977] and subdivided into assemblages based on volcanological genesis and lithological characteristics. Some locations were mapped based on the

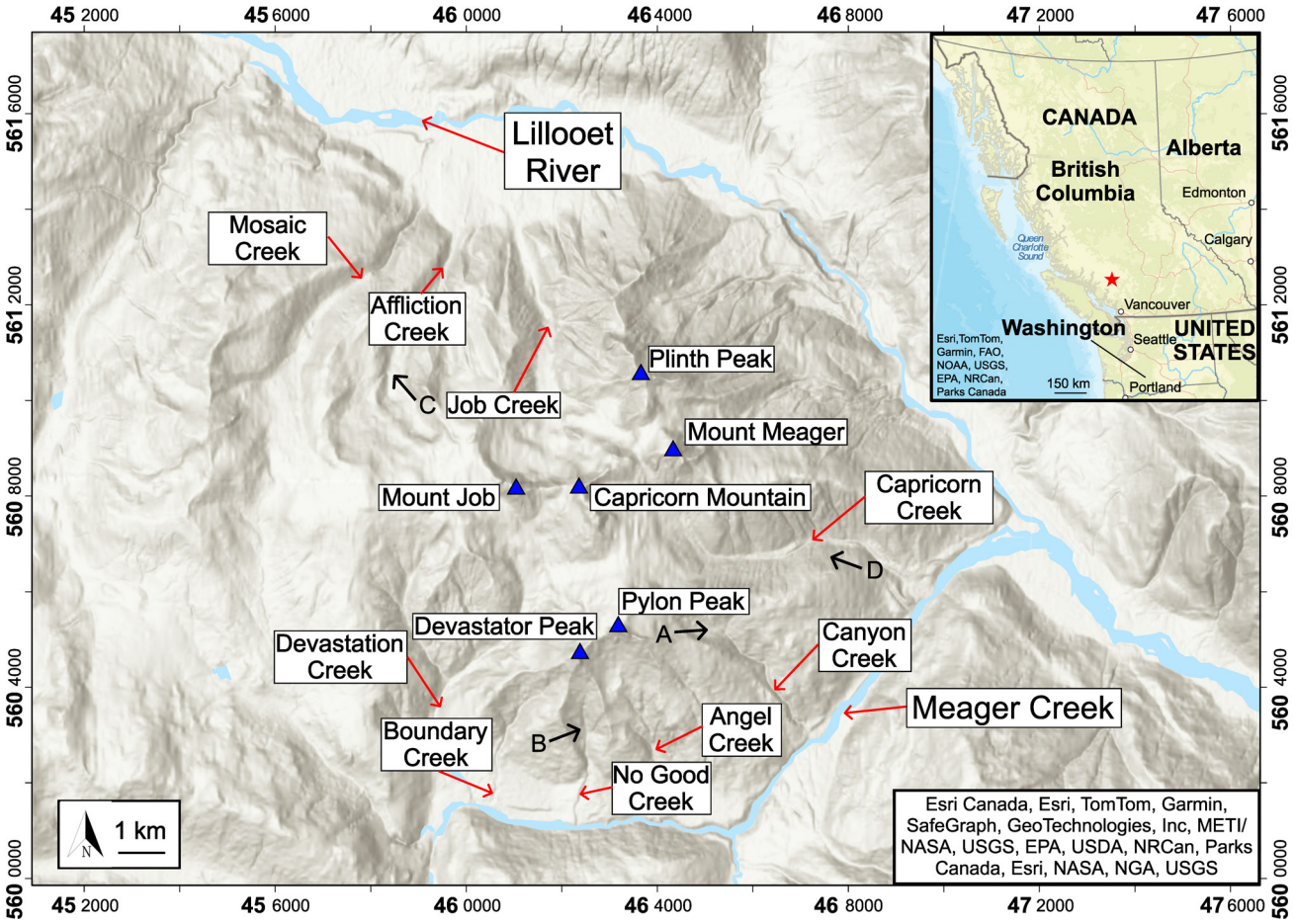

Figure 1: Overview of the Qwelqwelústen(Mount Meager Volcanic Complex), with major creeks and rivers (red arrows) and peaks (blue triangles) delineated. Coordinates in UTM Zone 10N, WGS 84. Lettered black arrows indicate photo locations from Figure 4.

surface material where bedrock was not visible, such as under glaciers or large landslide deposits. A simplified map showing volcanic assemblages was later generated [Read 1990]. Full label descriptions are provided below (Table 1). Fifteen volcanic assemblages were identified in the original mapping by Read [1977] and were further expanded during recent mapping [Stewart et al. 2008; Harris et al. 2021] (Figure 2). Volcanic units generally young northwards across the complex [Lewis et al. 1978; Muhammad et al. 2024]. Pliocene-aged units were identified dominantly in the southwest of the complex from an early period of rhyodacitic volcanism [Read 1990]. Pleistocene volcanic assemblages make up most of the complex with the youngest of these consisting dominantly of highly altered rhyodacitic tuff, breccia and flows from between 1.9 ± 0.2 Ma and 1.0 ± 0.1 Ma [Read 1977].

Much of the south and centre portion of the complex was formed following a shift to andesitic volcanism from 1.0 ± 0.1 Ma to 0.5 ± 0.1 Ma, with the Devastator Peak (Figure 1) being the primary source [Read 1990]. A late period of rhyodacitic volcanism from 0.1 ± 0.02 Ma to 2360 ± 50 BP produced the upper portions of many peaks observed today within the complex, including Mount Job, Capricorn Peak, Mount Meager, and Pylon Peak (Figure 1) [Hickson et al. 1999]. These units range from interglacial to postglacial with breccias, flows, and intrusions frequently encountered [Read 1977].

Volcanic rocks overlie Triassic to Miocene basement intrusive material and metamorphic material including quartz diorite, granodiorite, schist and gneiss [Read 1977; Harris et al. 2021]. Periods of dacitic, rhyodacitic, and andesitic volcanism occurred from around 1.9 Ma to 0.4 Ma [Read 1990]. A period of basaltic volcanism occurred on the massif between Job and Mosaic Creeks (Figure 1) and more broadly across the MMVC from 0.02 ± 0.06 Ma to 0.44 ± 0.10 Ma [Anderson 1975; Wilson and Russell 2019; Harris et al. 2023; Morison and Hickson 2023]. The most recent dated periods of explosive volcanism occurred during 24.3 ± 2.3 ka [Russell et al. 2021] and 2360 ± 60 ^{14}C BP [Clague et al. 1995; Hickson et al. 1999] on the northeast flank of Plinth Peak. The latter eruption generated pyroclastic density currents, lahars, and flooding after the failure of a welded block-and-ash flow created a dam that temporarily blocked the Lillooet River [Hickson et al. 1999; Stewart et al. 2008; Andrews et al. 2014].

Alpine glaciation occurred in the region beginning around 7–8 Ma [Denton and Armstrong 1969; Ehlers et al. 2006], with glacial erosion accelerating around 1.8 Ma [Shuster et al. 2005; Ehlers et al. 2006]. The Fraser glaciation is the most recent glacial episode in the southern Coast Mountains [Church and

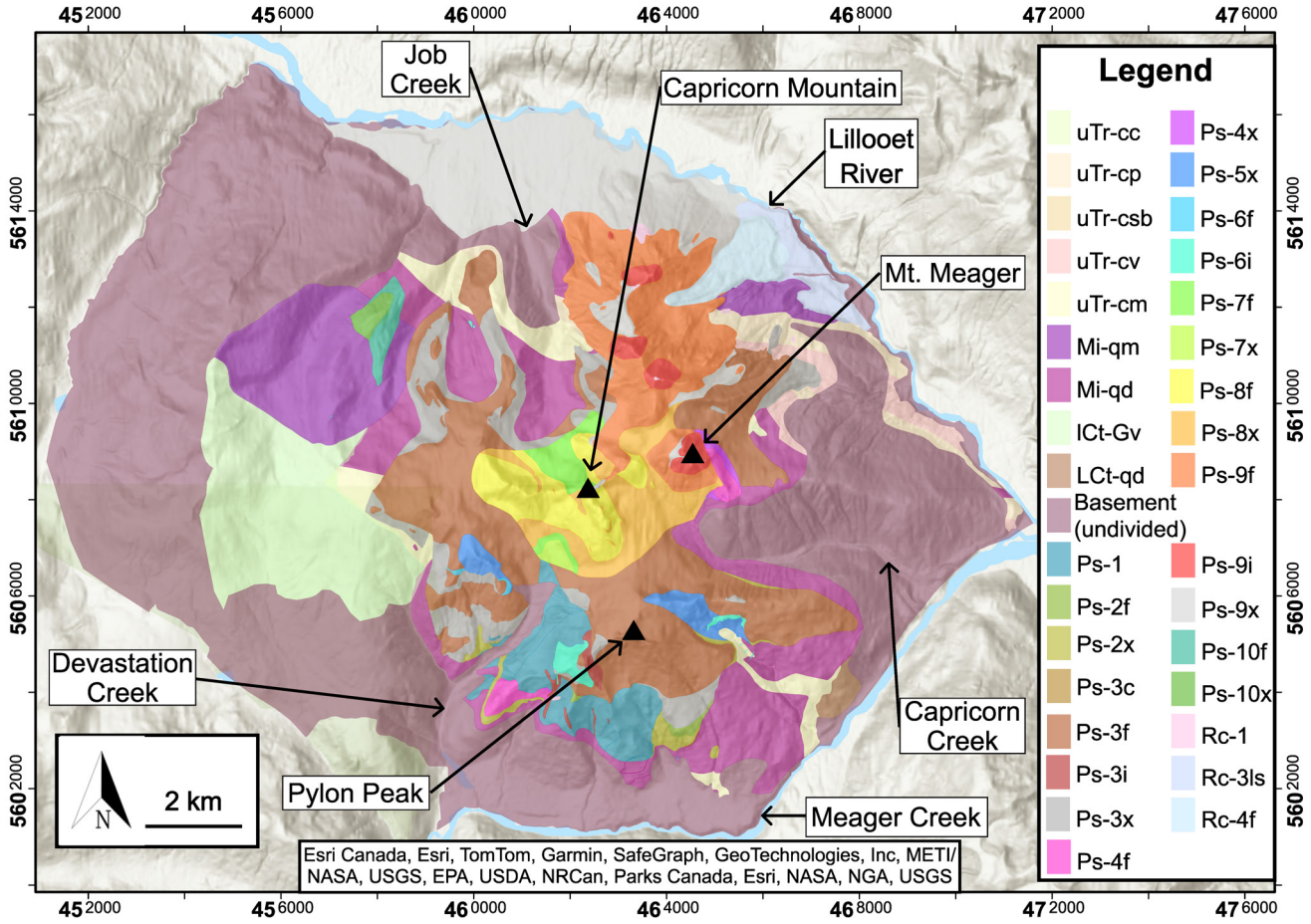

Figure 2: Detailed lithological mapping from the Q̓welq̓welústen (Mount Meager Volcanic Complex) [Read 1977; Harris et al. 2021]. Description of lithological units in Table 1. Coordinates in UTM Zone 10N, WGS 84.

Ryder 2010], spanning between 25,000 and 10,000 ^{14}C BP in British Columbia's mountains [Clague and Ward 2011]. Neoglacial ice advances from the Little Ice Age have left noticeable impacts in the valleys surrounding Q̓welq̓welústen. In the southern Coast Mountains, three phases of ice advance have been recorded, with the earliest being the Garibaldi phase (6000 to 5000 ^{14}C BP) and the latest occurring around 900 ^{14}C BP [Ryder and Thomson 1986]. Steep undercutting is frequently observed around neoglacial trimlines in the MMVC, more so than in nearby granitic basins [Holm et al. 2004].

The Q̓welq̓welústen area has long been a treasured area by the Líl̓wat First Nations for both its cultural and spiritual significance and the Nation has preserved many important oral histories including about its extensive hot springs [Jones 2011; Angelbeck et al. 2024] and even the most recent eruption in 2360 BP [Wilson et al. 2024]. The area has also been identified as a promising location for geothermal energy potential, with studies on the area having begun as early as 1975 [Jessop et al. 1991] and continuing in the southern part of the complex, near Meager Creek. A wide range of studies involving structural geology [Muhammad et al. 2024], geophysics [Klaasen et al. 2021; Lu and Bostock 2022; Hanneson and Unsworth 2023; Hormozzade Ghalati et al. 2023; Unnsteinsson et al. 2024], geological mapping [Harris and Russell 2021; Harris et al. 2021], volcanic hazards [Warwick et al. 2022; Kelman and Wilson 2024] and hydrogeology [Jamieson and Freeze 1982] have been completed on the complex, with the Garibaldi Geothermal Energy Project being the most recent multidisciplinary research endeavour [Grasby et al. 2021]. Pumice mines, hydroelectric projects and logging operations are all present on or around the Q̓welq̓welústen massif [Warwick et al. 2022].

3 Methodology

Statistical landslide susceptibility methods are based on the functional relationship between predictor variables and an inputted landslide distribution [Guzzetti et al. 1999]. These methods are based on the assumption that past factors governing landslide occurrence will likely control landslide occurrence in the future [Carrara et al. 1995]. Predictor variables used in statistical models commonly include geological, hydrological, land cover, and morphological categories, with the most common predictor variables being slope, lithology, and aspect [Reichenbach et al. 2018]. The most significant predictor variables can vary depending on factors such as the type of landslide being studied [Liang et al. 2021]. Studies dividing an area of interest into domains also found similarities and differences between predictor variable importance amongst the different domains [Petschko et al. 2014]. Statistical landslide suscepti-

Table 1: Lithological unit descriptions [Read 1977] included in this study and shown in Figure 2.

Label	Colour	Description
uTr-cc		White marble
uTr-cp		Grey phyllite; minor greywacke
uTr-csb		Biotite muscovite schist and gneiss
uTr-cv		Greenstone, volcanic breccia
uTr-cm		Streaky amphibolite
Mi-qm		Biotite quartz monzonite
Mi-qd		Biotite hornblende quartz diorite
lCt-Gv		Aphanitic grey-green flows, tuff and breccia with granitic detritus
Lct-qd		Biotite quartz hornblende quartz diorite
Basement		Basement rock (undivided)
Ps-1		Devastator assemblage: White, altered rhyodacite tuff, breccia and flows
Ps-2f		Dark grey, aphanitic andesite flows
Ps-2x		Andesite breccia and ash
Ps-3c		Andesite (Pylon assemblage)
Ps-3f		Pylon assemblage: Porphyritic andesite flows
Ps-3i		Pylon assemblage: Porphyritic andesite
Ps-3x		Pylon assemblage: Porphyritic andesite flows
Ps-4f		Porphyritic andesite breccia
Ps-4x		Porphyritic andesite flows
Ps-5x		Porphyritic andesite breccia and tuff
Ps-6f		Light grey, porphyritic andesite flows
Ps-6i		Light grey, porphyritic andesite
Ps-7f		Job assemblage: Ochre weathering, porphyritic rhyodacite flows
Ps-7x		Job assemblage: Ochre weathering, porphyritic breccia and ash
Ps-8f		Capricorn assemblage: Dark grey to purple, porphyritic rhyodacite flows
Ps-8x		Capricorn assemblage: Dark grey to purple, porphyritic rhyodacite breccia and ash
Ps-9f		Plinth assemblage: Light to medium grey, porphyritic rhyodacite flows
Ps-9i		Plinth assemblage: Medium to dark grey, porphyritic rhyodacite
Ps-9x		Plinth assemblage: Light to medium grey, porphyritic rhyodacite breccia and ash
Ps-10f		Mosaic assemblage: Porphyritic basalt
Ps-10x		Mosaic assemblage: Vesicular to scoriaceous basalt, breccia, tuff and bombs
Rc-1		Pebble Creek formation: Blocks and ash of porphyritic rhyodacite pumice
Rc-3ls		Pebble Creek formation: Landslide or lahar debris derived from unit Ps-9f
Rc-4f		Pebble Creek formation: Light grey, porphyritic rhyodacite vitrophyre

bility studies are quantitative, generating numerical estimates of landslide occurrence [Guzzetti et al. 1999], and as such can be implemented as machine learning models. These methods are also indirect, estimating susceptibility based on the relationship between predictor variables and an inputted landslide distribution [van Westen et al. 2003]. When used in a predictive manner, results are based on the assumption that the factors controlling the occurrence of previous landslides also control the occurrence of future landslides [Guzzetti et al. 1999]. In this study we use logistic regression and random forest methods, which are among the most common techniques for statistical landslide susceptibility analyses in different geological contexts [Sun et al. 2021; Barman et al. 2023].

3.1 Modelling methods

3.1.1 *Logistic regression*

Logistic regression is a widely used statistical method for analyzing the response between one or more outcome variables and a series of predictor variables known in the statistical field and henceforth referred to as features. Logistic regression is commonly used in landslide susceptibility mapping [Brenning 2005; Budimir et al. 2015; Lombardo and Mai 2018; Reichenbach et al. 2018], where the occurrence or absence of landslides is denoted by a 1 or 0. Binary logistic regression is built upon the assumptions of independent observations, non-perfect collinearity in features, and linearity between continuous features and the transformed outcome [Harris et al. 2021].

The Least Absolute Shrinkage Selection Operator (LASSO) logistic regression [Tibshirani 1996] is a form of penalized logistic regression that has been applied successfully to many landslide susceptibility studies [Camilo et al. 2017; Lombardo and Mai 2018; Amato et al. 2019]. The method reduces variance in a logistic regression model by using a penalty parameter λ to apply a small amount of bias in the log-likelihood function (Equation 1). LASSO can reduce model coefficients towards or equal to zero [Tibshirani 1996], leading to a form of simultaneous feature selection [Zou and Hastie 2005]:

$$L_\lambda(\beta) = \sum_{i=1}^{n} \{y_i \ln [\pi(x_i)] + (1 - y_i) \ln [1 - \pi(x_i)]\} + \lambda_l \sum_{j=1}^{p} \beta_j \vee \quad (1)$$

where $L_\lambda(\beta)$ is the LASSO regression log-likelihood function, λ_l is the LASSO shrinkage parameter, $\pi(x)$ is the conditional mean, x_i the features for observation i of n and y_i is the outcome response for observation i of n.

3.1.2 *Random forest*

Random forest [Breiman 2001] is a tree-based statistical method that tends to generate models with low degrees of overfitting [Merghadi et al. 2020]. The method averages a series of decision trees derived with randomization. Randomization is applied in the original random forest algorithm [Breiman 2001] through the sampling technique [Breiman 1997] and random feature selection at each decision tree node [Amit et al. 1997]. Results from individual trees are aggregated by taking the mean for regression tasks or majority voting for classification tasks [Breiman 1996]. Many model properties can be tuned with hyperparameters. For this study, hyperparameters were used to control the number of features considered as splitting features at each split: the proportion of observations sampled and the minimum node size at which to split.

3.2 Statistical model workflow

3.2.1 *Modelling strategy*

Two iterations of statistical models were completed (Figure 3). Both logistic regression and random forest models were completed for each iteration, with logistic regression completed using the LASSO method. The goal of the first iteration was to assess the contribution of a wide range of factors and due to the large number of features in this model, the simplified lithology from Read [1990] was used. Following this step, a second model was generated with only the most significant features determined based on the first iteration model results to reduce overfitting and generate more interpretable results. Smaller models are often seen as more meaningful compared to those with a very large number of features [Guzzetti et al. 2006].

Both model iterations were generated with nearly identical workflows. A grid cell mapping unit was selected with grid cells generated at spatial resolutions of 5 m. For both logistic regression and random forest models, a classification framework was selected and generated models aimed at classifying pixels as either landslides or non-landslides. Probabilities generated from this framework describe the likelihood of being classified as either a landslide pixel or non-landslide pixel based on the inputted database of previous landslides and features. Logistic regression calculates this value as the conditional mean of the probability of belonging to a set class, calculated using the predictor feature values and fitted regression coefficients [Hosmer and Lemeshow 2000]. In random forest classification tasks, probabilities are calculated based on the proportion of trees voting for a class [Breiman 2001]. Non-landslide points were downsampled to obtain a recommended dataset balance for rare-event studies and weights were used to increase the importance of classifying the minor class values correctly. Each model was split into a training dataset consisting of 70 % of data and a testing dataset with the remaining 30 %. To assess variations that could be caused by the testing/training data split, as well as variation due to the downsampling of non-landslide data points, 500 iterations of both the logistic regression and random forest models were completed. Detailed workflow steps are described in subsequent sections.

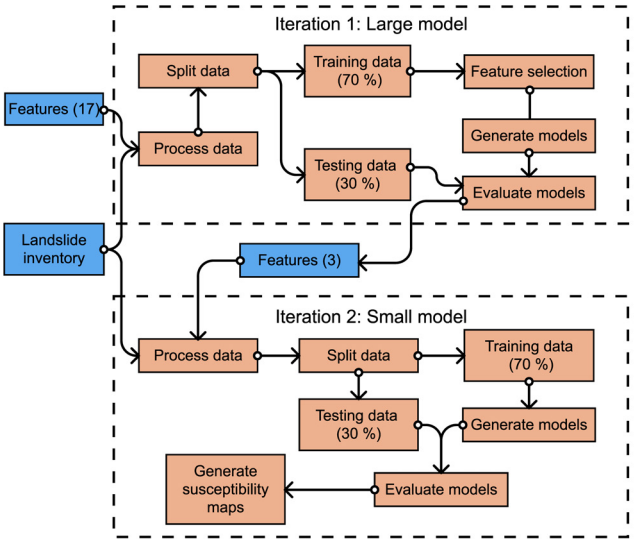

Figure 3: High-level workflow for the study.

Seventeen features were included in the large model and covered hydrological, geological, morphological, land cover, and climatic data categories (Figure 2). These features were derived from 1-m spatial resolution LiDAR acquired in 2015–2016 [Roberti 2018], satellite imagery [Planet Labs 2018], government sources [Natural Resources Canada 2019], or digitized from existing maps [Read 1977; Read 1990; Jordan 1995; Baumann Engineering 1999; Bovis and Jakob 2000; Roberti 2018].

3.2.2 *Data processing*

Prior to performing the statistical analysis, the data were analyzed to ensure the assumptions of logistic regression were met. Continuous data were assessed for highly correlated features using the Pearson's correlation coefficient. Through this process, Mean Annual Temperature and Terrain Ruggedness Index were removed from the dataset for subsequent models. The logistic regression assumption of independence was met by only selecting one data point from each landslide event. Values were taken as the mode for categorical data and median values for continuous data of pixels in the landslide source zone.

The logistic regression assumption of linearity in continuous features was assessed using the Box-Tidwell test [Box and Tidwell 1962], which assesses the relationship between log-transformed odds and continuous features. Features with a statistically significant relationship ($p < 0.05$) remained in

Table 2: Feature data summary

Features	Acronym	Random forest form	Logistic regression form
Aspect (°)	-	Continuous	Discretized
Elevation (m)†	-	Continuous	Continuous
Land cover (-)	-	Discretized	Discretized
Lithology (-)†	-	Discretized	Discretized
Mean annual precipitation (mm yr^{-1})	MAP	Continuous	Discretized
Normalized difference vegetation index (-)	-	Continuous	Discretized
Planar curvature (-)	PLC	Continuous	Discretized
Profile curvature (-)	PRC	Continuous	Discretized
Distance from roads (m)	RD	Continuous	Discretized
Slope (°)†	-	Continuous	Continuous
Stream Power Index (-)	SPI	Continuous	Continuous
Topographic Position Index (-)	TPI	Continuous	Discretized
Distance from trimlines (m)	TD	Continuous	Discretized
Topographic Wetness Index (-)	TWI	Continuous	Continuous
Distance from watercourse (m)	WD	Continuous	Continuous

† Variable used in both iterations of models

Table 3: Discrete data from first iteration (large) model. Lithology from Read [1990].

Feature	Label	Description
Land cover	SNF	Sub-polar taiga needleleaf forest
Land cover	TDF	Temperate or sub-polar broadleaf deciduous forest
Land cover	Mixed forest	Mixed forest
Land cover	TS	Temperate or sub-polar shrubland
Land cover	TG	Temperate or sub-polar grassland
Land cover	Barren land	Barren land
Land cover	Urban	Urban
Land cover	Water	Water
Land cover	Snow and ice	Snow and ice
Lithology	PL1	Basal breccia
Lithology	PL2	Porphyritic (quartz) dacite
Lithology	P1	Devastator assemblage
Lithology	P2	Pylon assemblage, aphanitic flows
Lithology	P3	Pylon assemblage, porphyritic plagioclase andesite
Lithology	P4	Job assemblage
Lithology	P5	Capricorn assemblage
Lithology	P6	Plinth assemblage
Lithology	P7	Mosaic assemblage
Lithology	R1	Pebble Creek formation
Lithology	Basement	Basement rock (undivided)

continuous form, while those with an insignificant relationship were transformed using the square, square-root and log functions and re-assessed. If no transformed features passed the Box-Tidwell test, features were discretized using breakpoints (Table 2). Discrete data labels are described in Table 3. Additionally, continuous features that lacked physical meaning over their entire scale were discretized, for example distance from roads and from neoglacial trimlines. Logistic regression features were standardized and centred such that output coefficients could be compared amongst features. The above transformations and discretizations were only completed for logistic regression modeling. Features were left in continuous form for random forest models. Further details on data processing are given in Supplementary Material 1.

3.2.3 *Statistical analysis*

Hyperparameters were tuned for the random forest model using a sequential model-based Bayesian optimization [Probst et al. 2019], with out-of-bag predictions used for evaluation. Model predictions were used during tuning, generating a much faster tuning process than other resampling techniques [Probst et al. 2019]. Hyperparameters tuned were the number of features which can be split at each node (from 0 to the maximum number of features), the minimum node size

to split at (from 0 to 140), and the fraction of observations sampled without replacement (from 20 to 90 %). Ranges were calculated using the recommended values [Probst et al. 2019]. The area under the Receiver Operating Characteristic curve (AUC) metric was used to evaluate results during hyperparameter tuning. The number of trees was set to 1000 because higher values often lead to increased model accuracy and more stable feature importance estimates [Probst et al. 2019]. For logistic regression models, the only hyperparameter tuned was the penalty coefficient λ. While random forest models have some degree of intrinsic feature selection [Louppe 2015], additional feature selection was performed to completely remove the least significant features as in the LASSO regression. This was completed by retaining the most significant 60 % of features using an AUC filter. The percentage of features retained was selected such that a comparable number of features remained as in logistic regression models (see Supplementary Material for further details).

The impact of individual features on logistic regression model predictions was quantified using the resulting beta coefficients output from the models. Random forest feature importance was calculated using the *Gini impurity*. The Gini impurity [Gini 1912] belongs to the Mean Decrease Impurity class of methods which quantifies importance based on the weighted impurity reduction from all nodes of the feature of interest, averaged over all trees [Scornet 2020]. Many statistical metrics were used to evaluate model quality on both testing and training datasets. Receiver Operating Characteristic curves are one of the most frequently used methods for describing model performance [Reichenbach et al. 2018]. The area under the Receiver Operating Characteristic curve (AUC) ranges from 1 (perfect predictor) to 0.5 (random predictor). Other metrics evaluated include the classification error, Binary Brier score and balanced accuracy.

Susceptibility maps were generated based on the mean probability for each pixel over all 500 model iterations. Standard deviation (SD) was also calculated for the probabilities, providing another indicator of variability between model results. Partial dependency plots are visual tools showing the effect a small number of features have on the estimated outcome [Friedman 2001] and can be used to estimate feature importance [Greenwell et al. 2018] on a wide range of statistical model types; these were generated using the `DALEX` package in `R` [Biecek 2018] for both logistic regression and random forest.

3.3 Landslide inventory generation

The landslide inventory was generated using a combination of images from helicopter overview flights (Figure 4), optical and radar satellite imagery, images from ground-based field work and previously published results in the literature [Mokievsky-Zubok 1977; Jordan 1995; Bovis and Jakob 2000; Friele et al. 2008; Guthrie et al. 2012; Roberti 2018]. Landslide events included in the inventory were restricted to slides or avalanches of either soil or rock according to the updated Varnes landslide classification system [Hungr et al. 2014]. This aims to simplify the range of mechanisms involved, which produces additional uncertainty in the statistical analysis. Nevertheless, some additional error will likely arise due to multiple types of landslides present in the inventory.

Only landslides with a minimum width of 30 m across the flanks of the mapped source zone were included in the study; minimum area thresholds have been used in other studies [Millard et al. 2002]. Prehistoric events not identified in the field were not included in the inventory since many are difficult to identify visually, and a detailed study focusing on landslide identification using landslide deposits was not conducted. In total, 117 landslides were identified for the inventory.

4 Results

4.1 Large model results and feature selection for small model

The results of the first iteration (large model) are shown in Figure 5, in terms of the feature inclusion of the features considered. Feature inclusion is calculated as the total number of models with the feature of interest after feature selection, divided by the total number of models (n = 500). Features that are more frequently selected during the feature selection process are more influential for predicting landslide susceptibility. Features included in a high percentage of models are also influential regardless of the database split and selected non-land slide points.

Feature selection for the small (second iteration) model was done using feature inclusion results from the large models (Figure 5) and manual inspection. Many features were consistently removed from models during automated feature selection. For logistic regression, these include aspect, Stream Power Index (SPI), Topographic Position Index (TPI), distance from trimlines, distance from watercourses, and Topographic Wetness Index (TWI). For random forest, aspect, Normalized Difference Vegetation Index (NDVI), Topographic Position Index (TPI), distance from watercourses, planar curvature, and profile curvature were frequently removed. Slope, elevation, land cover, mean annual precipitation, and lithology were frequently included in models in both logistic regression and random forest.

Based on the logistic regression results, mean annual precipitation was excluded from the model due to inconsistency between model results and the expected behaviour. The highest range of mean annual precipitation (map.3) resulted in a decrease in landslide susceptibility, while the intermediate range (map.2) resulted in an increase. Higher precipitation values would be expected to generally increase landslide susceptibility [Wang et al. 2020] and due to the misalignment between mechanism and result, it was excluded from the second iteration model.

Land cover was also excluded from the second iteration model as logistic regression results indicated that the only category which remained in greater than 50 % of models was barren land. This category may indicate that unvegetated slopes are more prone to landslides. However, it may also be a result of landslide source zones being unvegetated due to the landslide events, as most landslides had occurred prior to land cover mapping. The snow and ice category was the only other category included in a significant number of logistic regression models (Figure 5), being included in just below 50 %

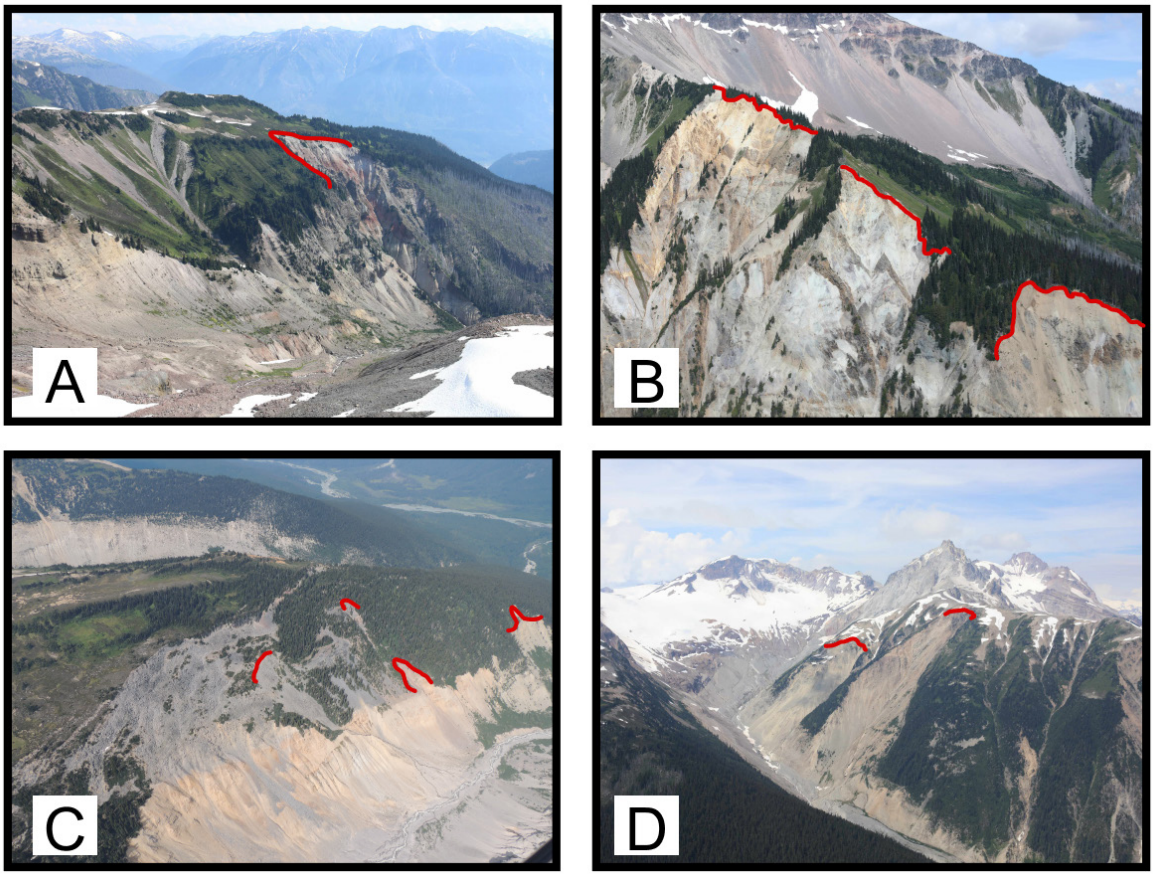

Figure 4: Landslides from [A] Canyon Creek basin, [B] No Good Creek basin, [C] Affliction Creek basin and [D] Capricorn Creek basin. The large block field in [C] is part of a deep-seated gravitational landslide [Bovis 1982; 1990]. Red lines depict the landslide crowns. Photo locations are shown in Figure 1. Photos by B. Coughlan and J. Connelly.

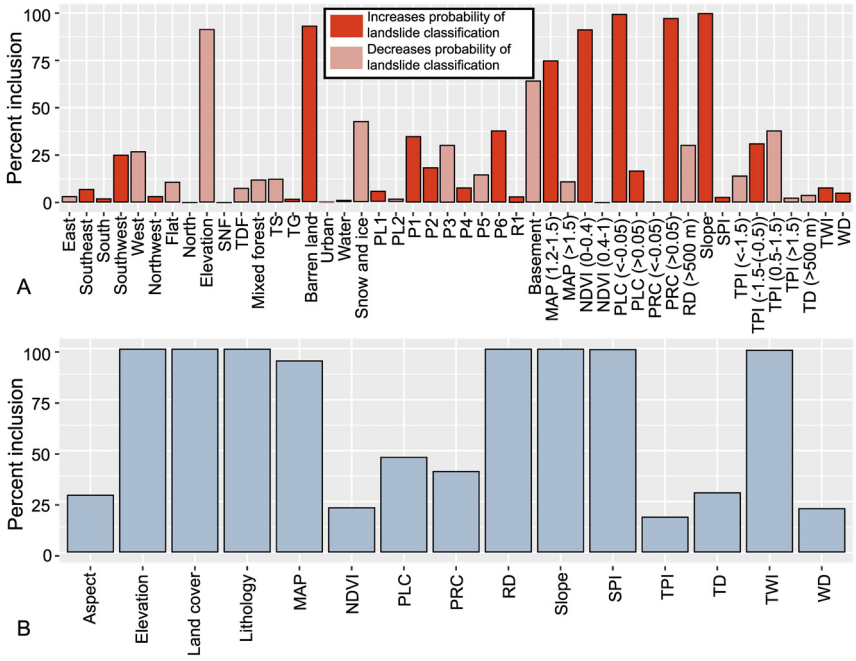

Figure 5: Large model feature importance results for [A] logistic regression and [B] random forest. Full feature descriptions can be found in Table 2 and Table 3.

of models. The feature was not included in the subsequent iteration because of the lower logistic regression inclusion relative to other features of interest and to restrict the second iteration model to only the most critical features. Slope, elevation, and lithology were the final parameters chosen for the subsequent iteration (small model).

4.2 Small model results and feature importance

The small (second iteration) model allows a more detailed assessment of feature importance, notably the slope, elevation, and lithological units. Feature importance metrics (Figure 6) provide insight to the extent a given feature contributes to the model. Figure 6 shows standardized absolute beta coefficients for logistic regression and importance values estimated using the Gini impurity for random forest models for the small model. Lithologies removed in all logistic regression models during feature selection are not shown. In both model types, slope is clearly the most important feature. Elevation is more significant in logistic regression models, with all lithology categories averaging smaller beta coefficients. In random forest, lithology ranks marginally higher compared to elevation. For a representative comparison between logistic regression and random forest lithology results, individual categories of lithologies should be compared. While this is not possible using the importance metrics shown here, it is possible using partial dependency plots (Section 4.3).

Beta coefficients for all basement material units result in a reduction in landslide susceptibility (Figure 6). Half (9/18) of logistic regression beta coefficients increased the likelihood of landslide classification with the largest coefficients with significant inclusion being Mi-qm (biotite quartz monzonite), Ps-1 (Devastator assemblage), and Ps-9x (Plinth assemblage).

4.3 Partial dependency plots

Partial dependency profiles (Figure 7 and Figure 8) illustrate how the average prediction varies over the features range of values. Slope values alter the average prediction by large amounts, indicated by the steep slope in the partial dependency profiles. The logistic regression slope profile increases at a more uniform rate compared to that of random forest, which increases rapidly between 20 and 50°. This is likely due to the flexibility of random forest compared to logistic regression. Elevation profiles exhibit similar trends. Both indicate landslide susceptibility is generally lower at higher elevations, however the logistic regression profile is much more linear and subdued, while the random forest profile captures many small variations. Note that logistic regression slope values are square root transformed on the x-axis to meet the logistic regression assumption of linearity.

Categorical random forest partial dependency profiles for lithology (Figure 8) appear very different for logistic regression and random forest. Partial dependency results for logistic regression lithologies that were removed during feature selection from all 500 models are not plotted. Logistic regression values deviate little from the mean value with changes in lithology and indicate that Ps-1 (Devastator assemblage) and Ps-9i (Plinth assemblage) are the most susceptible units. Logistic regression partial dependency plots do not indicate any units are of particularly low susceptibility.

Changes in lithology vary with average predictions much more significantly in random forest models. Results indicate Ps-1 (Devastator assemblage), Ps-9i (rhyodacite of Plinth assemblage), Ps-9f (rhyodacite flows of Plinth assemblage), and Ps-10f (basalt of the Mosaic assemblage) are the most susceptible units. Least susceptible units are uTr-cp (grey phyllite with minor greywacke, basement rock), Ps-3c (Pylon assemblage), Rc-4f (Pebble Creek Formation), and uTr-cv (greenstone and volcanic breccia, basement rock).

Both methods of analysis indicate Ps-1 (Devastator assemblage) and Ps-9i (rhyodacite of Plinth assemblage) are high-susceptibility units. No clear correlations between random forest and logistic regression exist for low-susceptibility units, partly due to the very low variation in logistic regression average predictions.

4.4 Model validation

Receiver Operating Characteristic curves generated on testing datasets (Figure 9) highlight some differences between model iterations and model types. Random forest models (AUC = 0.874) obtained marginally higher AUC values than logistic regression (AUC = 0.860) for the larger iteration. The same pattern held true for small models (AUC = 0.822 and 0.806). While these scores are considered excellent by some standards [Mandrekar 2010], most statistical landslide susceptibility studies result in AUC values greater than 0.8 [Fleuchaus et al. 2021]. Receiver Operating Characteristic curves manifest themselves similarly, with small deviations. The large random forest model appears to most outperform logistic regression at high sensitivity values while the small model random forest outperforms logistic regression most at lower sensitivity values.

Variation in training and testing performance results for the second iteration of models is shown in Figure 10. There are many consistent trends between the various metrics. In most metrics, there is a large performance variation between training and testing datasets in the random forest models, resulting in high model variance. The logistic regression model performance decreases only slightly with the shift from training to testing datasets due to the bias inserted into the model as part of the LASSO regression process. Even with the high levels of variance, random forest testing results exceed those of logistic regression. Note that training metrics shown were evaluated on a biased dataset and provide no indication of model performance.

4.5 Susceptibility maps

Susceptibility maps were generated for the second iteration model based on aggregated prediction results from all 500 model repeats. Typical values are shown by the calculated means while variation between the 500 repeats is delineated using standard deviation values (Figure 11). Predicted values for logistic regression are much closer to the central probability (0.5) compared to that of random forest as indicated by the histograms, and darker shades in the random forest mean plot. Random forest classifies most pixels with very low land-

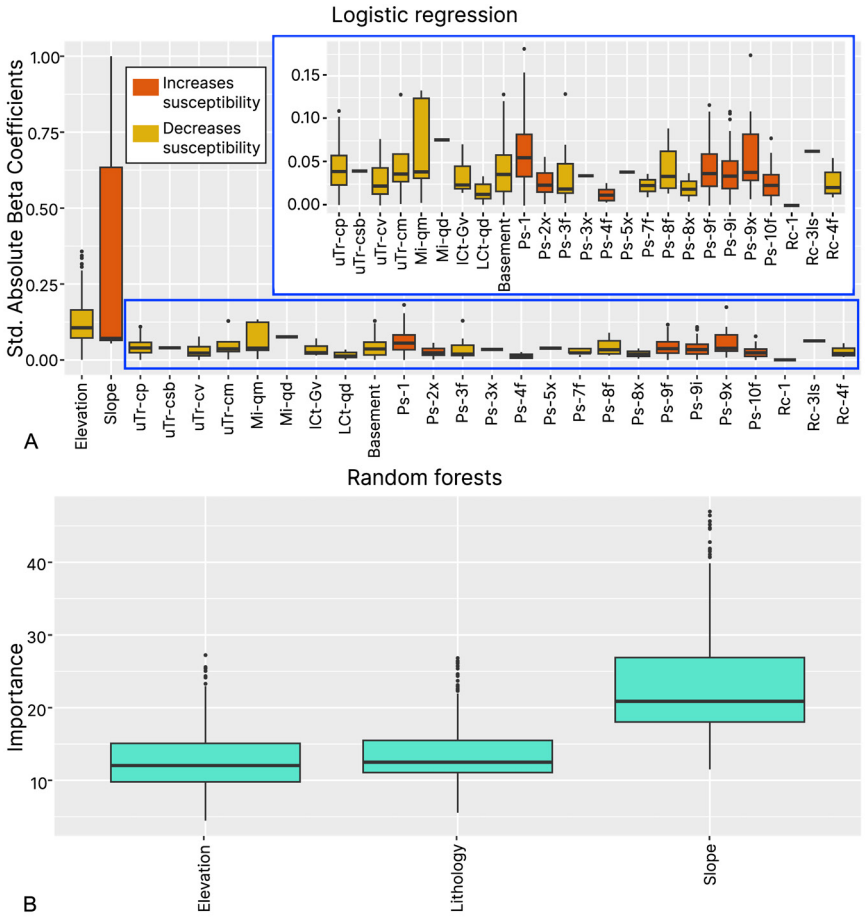

Figure 6: Feature importance results for [A] logistic regression and [B] random forest.

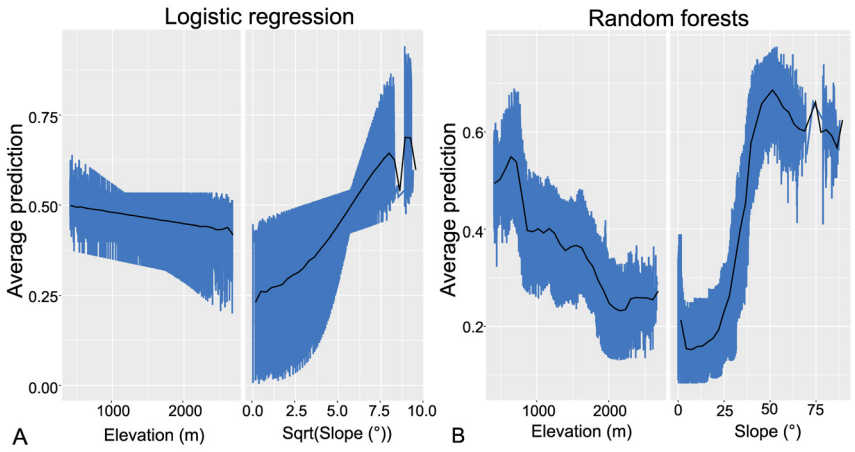

Figure 7: Continuous feature partial dependency profiles for [A] logistic regression and [B] random forest for elevation and slope features.

slide probabilities, as would be expected. More pixels in the map also have very high probabilities, indicated by the darker red shades. Logistic regression has a much more uniform distribution in standard deviation (SD) values, with most pixels having a low SD and the frequency decreasing as the SD increases. Intermediate SD pixel values are most frequent in the random forest model, however very high standard deviations are less frequent than logistic regression.

Geomorphic trends are generally similar between both mean predicted probability plots. Both models predict steep valley sidewalls as generally being of high susceptibility, along with other steeper slopes such as along rivers. The increased influence of lithology in the random forest model can be seen from lithological contacts in the susceptibility maps along units such as the Devastator assemblage (Ps-1; 1 in Figure 11), basement units (uTr-cm; 2 in Figure 11), and along basement-

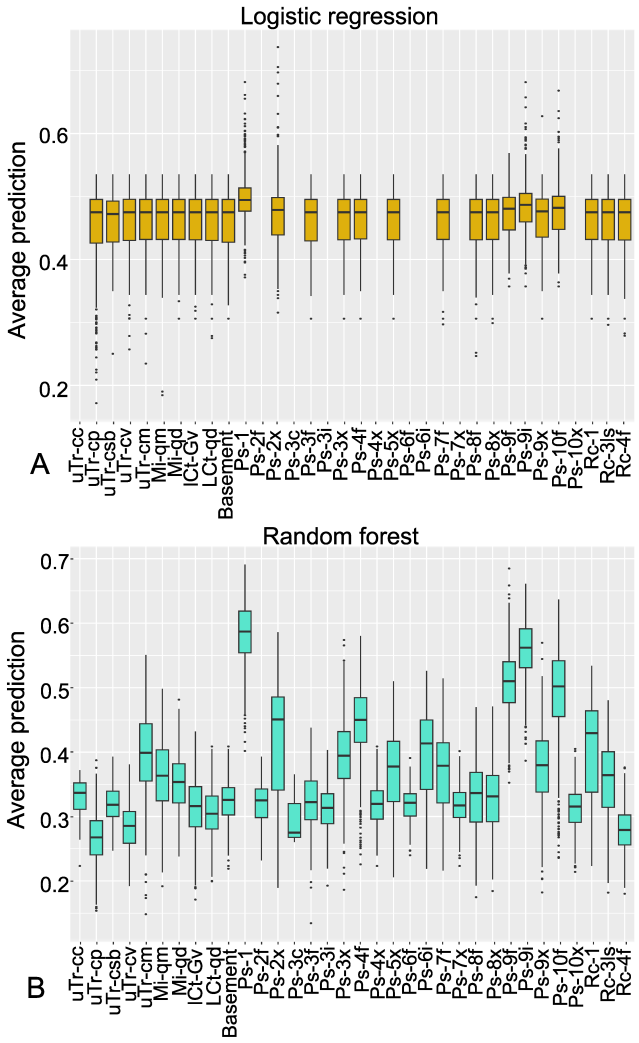

Figure 8: Categorical partial dependency profiles for lithology using [A] logistic regression and [B] random forest. Features not plotted in [A] were removed during feature selection for all 500 models.

volcanic contacts (Ps-3f and Mi-qd; 3 in Figure 11) amongst others. Unit outlines can be seen in the random forest susceptibility map (Figure 11B), delineating changes in prediction based on lithological unit while they are much more difficult to observe in the logistic regression map (Figure 11A).

Both logistic regression and random forest methods indicate steep slopes, such as glacially oversteepened valley sides, typically also have larger SDs than other nearby areas (Figure 11C, 11D). In many aspects, the distribution of SD values varies greatly between logistic regression and random forest. Random forest SD has greater levels of variation with changes in lithological unit. In the southwest of the study area, many pixels have high SDs in logistic regression models, but very low values in random forest models likely due to lower lithological influence in the logistic regression model. A larger landslide dataset would likely help reduce some variation in random forest models, which appear to be influenced by the testing dataset split and non-landslide point downsampling to obtain the 5:1 landslide to non-landslide point ratio from the initial 59:1 ratio present in the raw data.

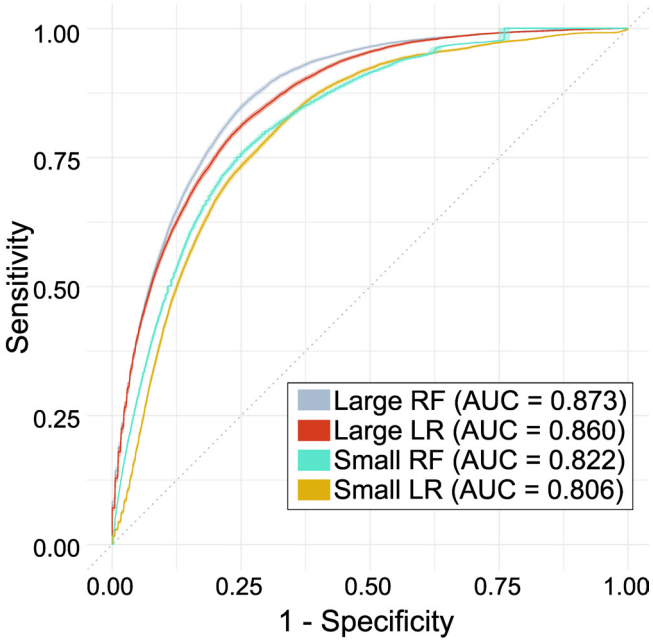

Figure 9: Receiver Operating Characteristic curve for all models generated from testing data.

4.6 Sources of error

There are a variety of sources of error that affect model results. Firstly, there is error in both main sources of input data. Landslide mapping was conducted using a variety of methods to minimize error. Some identified landslides were verified using previously published results, however, there may be some misidentified and excluded events. Based on characteristics of the massif, there is likely more error in results mapped on high slopes in the massif, where identification of landslides is more difficult due to a lack of vegetation, glacier coverage and frequent colluvial cover. Error association with input geomorphological features is generally small, as most features were derived from 1-m spatial resolution LiDAR resampled to a 5-m spatial resolution.

The analytical methodology also introduces some additional error. Only one point was selected to represent each landslide point to satisfy requirements of logistic regression. However, these may not be representative of the whole landslide body and is highlighted for cases where a landslide may occur over a source zone covered by multiple discrete categories. In these cases, only one category can be selected, resulting in an underrepresentation in the other category. The 2010 Mount Meager landslide is an example of such an event, that originated in two lithologies [Roberti 2018].

5 Discussion

The susceptibility analyses show that slope angle has the greatest control on landslides in the complex, as is evident in both linear Regression and random forest models. This aligns with expectations based on the physics of slope stability and results from other landslide susceptibility studies. The

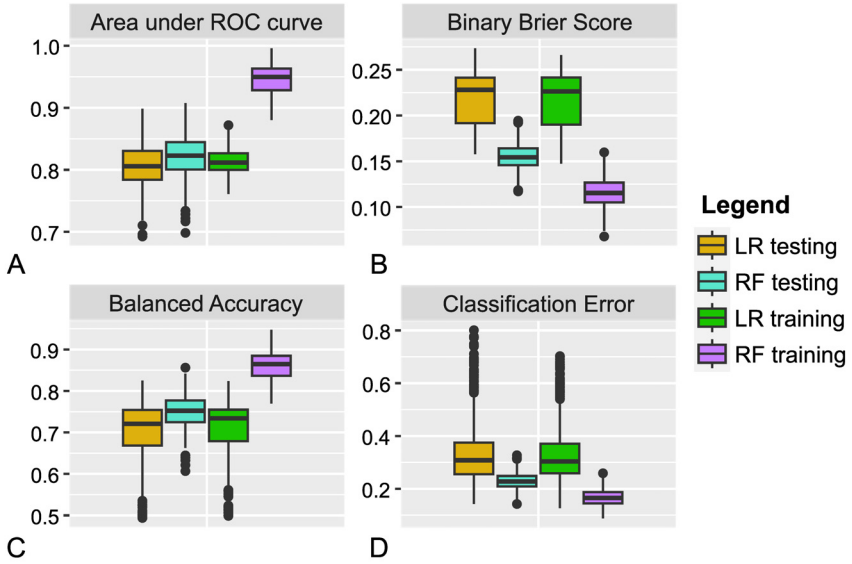

Figure 10: [A] Area under the Receiver Operating Characteristic curve, [B] binary Brier score, [C] balanced accuracy and [D] classification error for all models.

majority (95 %) of studies recorded slope as the most significant feature [Budimir et al. 2015]. At Q̓welq̓welústen/MMVC, landslide susceptibility generally decreased with increasing elevation. This trend could be due to less landslides in the upper peaks of the massif due to glacier cover, or increased smaller volume landslides at lower elevations along waterways where stream power is larger. The former explanation is more likely, as landslides have previously occurred under glacier cover at the massif [Mokievsky-Zubok 1977] and other volcanoes [e.g. Huggel et al. 2008]. Upper portions of the massif also have more uncertainty in landslide mapping results. The third group of significant features is lithology, which have some distinct characteristics in a volcanic massif compared with landslide studies elsewhere.

5.1 Lithological influence on landslides

Model results indicate that the crystalline basement material tends to decrease landslide susceptibility, while volcanic material is likely to lead to increases. All logistic regression beta coefficients for basement material suggested decreases in landslide probability, while half of the volcanic assemblages increased the probability of classification as landslide susceptible. Both units of high landslide susceptibility in logistic regression partial dependency profiles are also volcanic. Random forest results indicate two of the four lowest susceptibility units were basement material. One of the two lowest susceptibility volcanic units (Ps-3c) covers a very small area, which likely led to an inadequate sample size for the unit. All eight of the highest susceptibility units determined using random forest partial dependency plots are volcanic. The combination of these results suggests that high-susceptibility units in the complex are volcanic, while there is more uncertainty classifying the lowest susceptibility units, which may be volcanic or basement rock with basement material being more likely.

Variations in groundwater flow patterns and pore pressure between basement and volcanic units could also play a role in varying landslide susceptibility between units. In volcanoes, porosity, fracturing, compaction, and the presence of clays can vary significantly resulting in a wide range of possible hydraulic conductivities [Mueller et al. 2005; Wright et al. 2009; Farquharson et al. 2015; Delcamp et al. 2016]. High thermal fluxes in volcanoes with large volumes of water also allow the hydrothermal system to expand, further weakening material [Delcamp et al. 2016]. Around Q̓welq̓welústen/MMVC, cold springs have been identified in volcanic, basement and unconsolidated material, and are likely stratigraphically controlled [Jamieson 1981]. Hydrothermal alteration in volcanic systems can alter porosity, resulting in variations in pore pressure which can induce volcano instability [Heap and Violay 2021]. High pore pressure due to water infiltration from snowmelt and permafrost thaw were a triggering factor in the 2010 Mount Meager landslide and resulted in fluid-rich phases of flow [Roberti et al. 2017].

Due to the complex processes occurring in volcanic centres, material is often highly heterogeneous with a wide range of properties [del Potro and Hürlimann 2008]. Volcanic material at the site dominantly consists of rhyodacitic to basaltic-andesitic flows, breccias, pumice, tuff, bombs, and pillow lava units [Read 1977; Read 1990]. Basement material is mostly quartz diorite [Read 1990], with metamorphic rocks such as schist, gneiss and amphibolite also present [Harris et al. 2021]. A multielement geochemistry study of the MMVC indicated that at least two periods of hydrothermal alteration have occurred [NSBG 1985]. An early period of alteration characterized by propylitic alteration and chalcopyrite affected basement material while a later alteration episode resulted in sphalerite, pyrite, clays, carbonates, and chlorite related to the current geothermal system affected both basement and volcanic rocks [NSBG 1985]. Studies have shown that alteration can result in increases or decreases in the strength of volcanic rocks [del Potro and Hürlimann 2009]. Alteration associated with a porosity decrease may increase rock strength [Heap et al. 2020], while alteration leading to an increase in porosity or formation of clays can reduce strength [del Potro and Hürli-

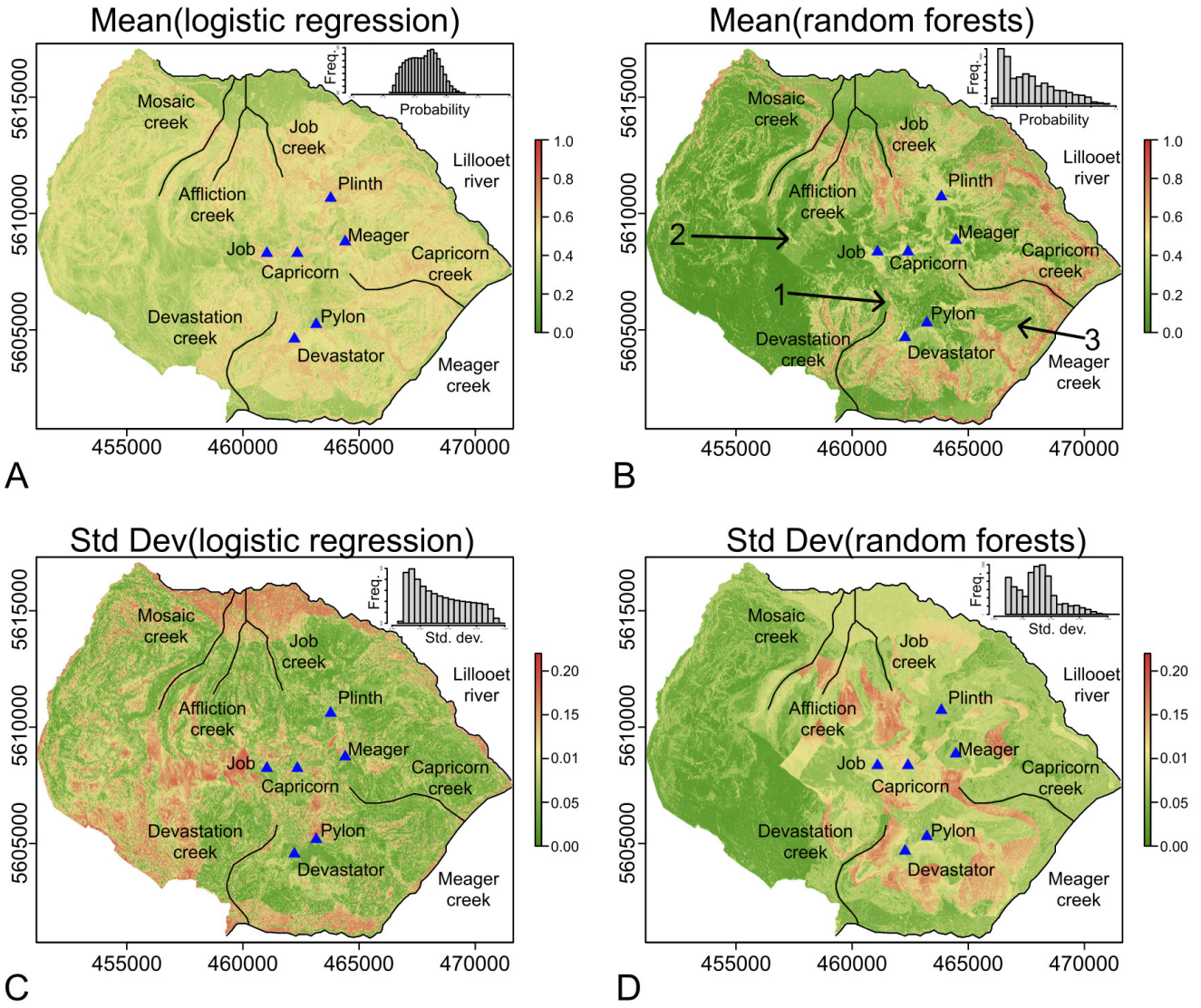

Figure 11: Susceptibility maps for second iteration models. Mean values are plotted for [A] logistic regression and [B] random forest with notable predictions as well as standard deviations for [C] logistic regression and [D] random forest. Histograms show the relationship between plotted values (x-axis) and frequency of occurrence (y-axis). Labelled locations in [B] refer to notable boundaries and are refered to in-text. Coordinates in UTM Zone 10N, WGS 84.

mann 2009; Frolova et al. 2021; Heap and Violay 2021]. Results from this study agree with these findings, with basement material being less susceptible despite possibly more alteration. The presence of clay minerals derived from the second stage of alteration is likely a major factor in the high susceptibility of the volcanic Devastator assemblage (Ps-1).

Both model types indicated that the early-Pleistocene Devastator and late-Pleistocene Plinth volcanic assemblages [Read 1990] are high-susceptibility lithologies. For logistic regression, this was concluded using both standardized beta coefficients (Figure 6) and partial dependency plots (Figure 8). Observations from other researchers support the Devastator assemblage as being of particularly high susceptibility. Read [1990] described the unit as intensely hydrothermally altered with ubiquitous clay minerals and many landslides consisting of the material. Portions of the Plinth assemblage around Pylon Peak (Figure 1) have undergone extensive hydrothermal alteration [Muhammad et al. 2024], which also likely contributes to the high levels of landslide susceptibility. This assemblage also comprised part of the source zone of the 53×10^6 m^3 landslide which occurred in 2010 on the flank of Q̓wel̓q̓welústen [Guthrie et al. 2012; Roberti 2018]. The Plinth assemblage is commonly vesicular, and contains diagnostic cognate inclusions of hornblende andesite [Read 1977; Read 1990]. The vesicular texture may lead to high porosity in the assemblage and a reduced intact rock strength [e.g. Entwisle et al. 2005; Aligholi et al. 2017]. Additional research on alteration levels and types in these units would be beneficial to these findings.

Point load testing of lava flow unit samples with differing alteration levels collected near Devastation Creek indicated very different strength levels. While the samples were taken far from the headwaters where the most intense alteration is observed, the less altered material had an estimated unconfined compressive strength of 123 ± 38 MPa while more altered samples yielded an unconfined compressive strength estimate of 73 ± 22 MPa. More altered samples also had much higher

porosity than unaltered samples. Based on these conclusions, it is likely that alteration associated with the geothermal reservoir, leads to higher landslide susceptibility due to the formation of clay minerals and a porosity increase. This is supported by geophysical research that has identified a conductive body spatially associated with the Devastator assemblage which is interpreted to be a clay-rich caprock layer [Hormozzade Ghalati et al. 2022]. This factor is likely combined at local scale with the rock mass structure, not analyzed in this regional-scale study, plus slope and elevation, to define the critical unstable areas within the most susceptible units.

While basement material may be less susceptible to landslides, our results indicate that basement rock can still be prone to failure. Both non-volcanic and volcanic factors affecting landslides may also affect basement material. Glacial retreat has been a major causative factor in multiple landslide studies surrounding Q̓welq̓welústen [Mokievsky-Zubok 1977; Bovis 1990], which affects both volcanic and basement material. Additionally, volcanic eruption centres have been strongly linked to basement tectonic features [Tibaldi et al. 2005]. At the Q̓welq̓welústen massif, fractures related to regional tectonic deformation are common in character between basement and volcanic material and are often in good alignment with volcanic eruption centres [Chen et al. 2021; Muhammad et al. 2024]. Thus, the rock mass structure in both basement and volcanic units may influence the occurrence of landslides. The Mi-qm basement unit is an example of a susceptible basement unit. In logistic regression studies, the magnitude of the beta coefficient is highly variable (Figure 6) and random forest results show the unit as being of moderate susceptibility, with the second highest average prediction for a basement unit (Figure 8). Portions of the unit outcrop along the valley walls of the recently deglaciated Mosaic and Affliction Creeks. Movement was detected in the Mosaic zone using differential interferograms [Roberti 2018] and the Affliction zone using ground-based field work [Bovis 1990]. Signs of deep-seated gravitational deformation are found throughout the complex, particularly along steep slopes high in the massif (such as Devastator Peak, Mount Meager, and Plinth Peak) and deglaciated valley walls.

Both highest landslide susceptibility lithologies (Plinth and Devastator) are located on slopes with geomorphological evidence of instability. Studies in these regions can be an additional form of validation for model results. The west flank of Plinth peak descends into the Job Creek basin and consists of altered material of the Plinth assemblage [e.g. Muhammad et al. 2024]. The site is considered one of the most likely sites for future edifice collapse [Friele et al. 2008; Hetherington 2014; Roberti 2018]. An optical monitoring camera was installed facing the slope, and has been used for motion detection with comparable results to InSAR measurements [Muhammad et al. 2022]. The upper portions of the Mount Meager peak also consist of material from the Plinth assemblage and has experienced multiple landslide events [Evans 1987; Roberti 2018], with the most recent and largest occurring in 2010 [Guthrie et al. 2012; Roberti 2018]. Signs of continued slope instability such as tension cracks remain even on the slope after the 2010 failure [Guthrie et al. 2012].

The northwest flank of the Devastator shows signs of slope instability [Roberti 2018] and is underlain by the Devastator assemblage. The slope is considered one of the most likely sites of edifice collapse [Friele et al. 2008]. Other locations with susceptible units and additional signs of instability include west-dipping slopes in Devastation Creek basin [van der Kooij and Lambert 2002; Friele et al. 2008] and areas with instability dominantly in basement material such as the east-dipping slopes in Affliction [Bovis 1982; 1990; Roberti 2018] and Mosaic [Roberti 2018].

5.2 Model performance

Random forest models recorded greater performance results in each metric. Small models resulted in AUC values of 0.822 for random forest and 0.806 for logistic regression, compared to 0.873 and 0.860, respectively, for large models. Many other studies have reported higher validation scores for random forest compared to logistic regression [Sahin et al. 2018; Merghadi et al. 2020; Akinci and Zeybek 2021; Chen et al. 2023]. The variation between results does vary depending on the metric. Random forest and logistic regression results appear closer in AUC and balanced accuracy, while random forest records significantly higher Binary Brier scores and lower classification error rates. Results highlight the need to assess models using multiple performance metrics.

Logistic regression and random forest training metric scores differ greatly. Random forest scores are very high when evaluating using the training data but decrease substantially when the testing dataset is evaluated. On the other hand, logistic regression scores show little decline when shifting from the training dataset to testing dataset evaluation. This indicates that the logistic regression model has very little overfitting and low model variance. The LASSO regression is known to provide this advantage [Tibshirani 1996]. Due to the high levels of variance, the random forest model is likely overfitting training data to some degree. Even with the overfitting, random forest still delivers higher performance results than logistic regression. The above findings are partly due to random forest being a more flexible method, able to capture more detail than logistic regression models. Partial dependency profiles from continuous features illustrate this point well (Figure 7).

The first iteration of models had a notable increase in performance compared to the smaller, second iteration. With the decrease in features, the logistic regression model recorded an AUC decrease of 0.054 and 0.051 for the random forest model. This indicates that decreasing the number of features had a consistent effect on logistic regression and random forest models and this decrease in performance can be explained by the chosen methodology. Gradient boosting algorithms train shallow decision trees sequentially and may yield improved results over random forest [e.g. Callens et al. 2020]. Multiple types of landslides were included to gather a sufficient size of landslide inventory; however, different landslides types have different physical behaviours, leading to different features in statistical studies best predicting their occurrence [Budimir et al. 2015]. The larger model likely contained some features that were best for classifying a subset of the landslide population, leading to higher scores in that model. Regardless of mecha-

nism, some other features may have very small effects, leading to higher scores in the large model.

5.3 Suitability of methods

Logistic regression and random forest provide a range of advantages and disadvantages, which were found to complement each other well. Logistic regression provides easy-to-interpret results but is not able to capture complex trends in the data. Models yielded improved results, however they are prone to overfitting as seen from the large model variance. Logistic regression partial dependency profiles yielded very little variation in average prediction for varying lithology, especially for low-susceptibility units. Differences in the influence of lithology between logistic regression and random forest models are likely caused by characteristics of the two methods. The LASSO logistic regression removed many categories of lithology from models during implicit feature selection, significantly reducing the average impact of most lithologies in partial dependency plots. This is due to regression coefficients for lithological categories generally being much smaller than that of slope. While decision trees do have some degree of implicit feature selection [Louppe 2015], the different mechanism leads to more variation in model importance results.

Higher model performance does not mean a model is necessarily the optimum choice for all landslide susceptibility objectives. Random forest models provided more insight on feature importance and were able to capture non-linear trends in continuous data. For these reasons, random forest is better suited for statistical landslide susceptibility studies aimed at evaluating feature impact and for studies involving complex relationships. Logistic regression models benefit from easy interpretation, very low degrees of overfitting and capturing main trends in data. Such advantages may be well-suited for a first-order susceptibility map and as a method of prioritizing zones for detailed study. Larger amounts of overfitting (as seen in the random forest models) can also produce results that are geomorphologically unreliable. Regardless of the chosen application, using multiple methods to validate results is the best practice.

Both methods benefit greatly from visual model interpretation tools, such as partial dependency plots (Figure 7 and Figure 8). This tool allows for a clear comparison of multiple methods, which otherwise may be challenging to compare and enable detailed interpretation of models that are conventionally more difficult to interpret, such as random forest. In this case, the impact of each discrete data class could be seen, which was not possible using the Gini impurity. Partial dependency profiles using a flexible method such as random forest would also be a useful decision-making tool when discretizing continuous features for use in logistic regression. Doing so would minimize information loss, one of the major disadvantages of discretization in statistical models.

5.4 Implications for hazard and risk

Model findings are in good agreement with previous studies of landslide hazards in the area [e.g. Baumann Engineering 1999; Friele et al. 2008; Friele 2012; Hetherington 2014; Roberti 2018]. Model results show that most glaciated valleys in the area are highly susceptible to landslides. Many unstable zones with monitored displacements and/or geomorphological signs of instability fall in the same valleys [e.g. Mokievsky-Zubok 1977; Bovis 1990; Roberti 2018; Muhammad et al. 2022]. As expected, most areas directly surrounding volcanic peaks are of high susceptibility, due largely to the steep relief associated with these features, combined with hydrothermal alteration of the volcanic rocks which may change intact rock strength [del Potro and Hürlimann 2009; Heap et al. 2020; Frolova et al. 2021; Heap and Violay 2021] as described above. Previous studies have identified the flanks of Plinth Peak and Devastation Peak as being of particular concern [Friele et al. 2008; Hetherington 2014; Roberti 2018]. Deep-seated gravitational movement is very common along valley walls in the massif [e.g. Bovis 1982; 1990; Bovis and Evans 1996; Hetherington 2014; Roberti 2018] and may evolve into more rapid failures, however many also remain stable within historical time [Hungr et al. 2014]. Findings from this study do give an indication of zones susceptible to initiation of events such as rock avalanches, although the study does not include deep-seated gravitational deformation zones that have not transitioned to such forms. Additional factors and temporal effects may also affect the evolution of deep-seated gravitational deformation into more rapid landslide forms, warranting a study of this process on its own.

Previous studies have shown that events originating high in the massif may have significant impacts to nearby infrastructure, most notably roads and bridges. Landslides in the complex have resulted in significant economic losses [Guthrie et al. 2012], fatalities [Mokievsky-Zubok 1977], and the temporary damming of nearby waterbodies [Evans 1987; Bovis and Jakob 2000]. High-susceptibility zones are in almost all major basins, although the Job Creek, Affliction Creek, Capricorn Creek, and Devastation Creek basins appear to have the largest susceptible zones. Results generally align with previous interpretations with hazards dominantly constrained to low-lying areas where landslide material may travel to or along [Baumann Engineering 1999; Friele 2012], and localized source zone slopes with highest risk zones in the south of the complex being along Devastation, Capricorn, and Meager Creeks [Baumann Engineering 1999]. The impact of an event would be dependent on properties of the landslide, such as its volume, initiation zone location, and the amount of water, ice and/or snow available, which may lead to fluidization of the initial rock slide and evolve into long-runout rock and ice avalanches and/or debris flows, as described in the previous examples. Large landslides also have the capacity to dam creeks, with the possibility of posterior breaching generating outburst floods. Landslides originating near higher order waterbodies may lead to localized road damages where road creek setback is small and possible temporary creek damming at narrow reaches.

Results from the models generated still require interpretation to produce commonly used maps such as risk or hazard maps. However, they demonstrate how quantitative results can be generated over a large area as a useful input for such assessments. Alternatively, model results can be combined with a variety of tools to predict runout hazards associated

with gravitational hazards [e.g. Horton et al. 2013; Mitchell et al. 2018; 2019].

These observations apply to the current geothermal lease area in the southern part of the study area, north of Meager Creek. The sector with potential industrial development falls mostly in moderate- to low-susceptibility areas, due likely to the occurrence of small, localized slope failures. Nevertheless, large avalanches or flows originating from Devastation or Capricorn Creeks may strongly impact accessibility to the site, affecting roads and especially bridges. Local debris flows in smaller creeks may also impede access at least temporarily. Furthermore, a hydroelectric facility is located along the Lillooet River in the northeast of the complex. Localized zones of high susceptibility along steep slopes are found near the development. Small landslides may occur here, likely with little impact beyond the source zones and immediate vicinity. More detailed smaller-scale investigations would be required to accurately characterize the stability of such zones, as small-scale effects such as jointing and variations in rock strength may dictate stability. Large-volume events leading to long runout flows may reach the area of development from high-susceptibility zones upstream of facilities. Plinth Peak and valley walls near Job, Affliction, and Mosaic Creeks are all susceptible to failure, and could travel past existing facilities situated near the Lillooet River. Such events may cause road access damages and implications for people nearby as well as damage to hydroelectric infrastructure.

6 Conclusions

Using cell-based statistical methods, landslide predictive factors were investigated on Q̓welq̓welústen/Mount Meager Volcanic Complex, a long-lived glaciated volcanic massif. Initial models considering a wide number of features determined that slope angle, elevation and lithology are the most significant features affecting inter-eruptive landslides in the MMVC. While logistic Regression models record lower performance results, these models also have much lower variance compared to random forest results. Results indicate many features are needed to capture the range of mechanisms observed in included landslide types.

All models show that the younger volcanic rock units tend to have higher susceptibility than basement rocks, with both materials having undergone similar morphological evolution and likely related to clay-rich, hydrothermal alteration processes. The Devastator and Plinth volcanic assemblages are of particularly high landslide susceptibility and results indicate the spatial association of the Devastator unit with a subsurface clay-rich cap layer also influences landslide susceptibility. Logistic Regression results show all basement lithologies decreased the probability of landslides, while 50 % of volcanic units increased the probability of landslide occurrence. Random forest model results show significant variation in average prediction with varying lithology, with all high-susceptibility units being volcanic and most low-susceptibility units being basement material. Findings agree with previous observations of volcanic rock being more susceptible to landslides and also show that high-susceptibility zones of basement material are present around the complex, particularly near glacial trimlines. As recognised by previous studies in the area, our results indicate that steep peaks on the massif, valley sidewalls, and slopes along higher order streams are of high initiation susceptibility. Most susceptible lithologies identified from model results align with expected zones based on monitoring and geomorphological observations, validating model results.

The findings from this study support the need for more detailed geologic mapping in volcanic environments as an input for landslide susceptibility and hazard assessments due to the impact of lithological factors and high degree of heterogeneity commonly observed in volcanic settings [del Potro and Hürlimann 2008]. Considering detailed lithological units in hazard mapping has implications for other uplifted volcanic massifs with glacial influences worldwide, such as in the northern Cascades Range, Japanese Alps, Caucasus region, Alaska, and the Patagonian Andes, amongst others. Better understanding and management of landslide risk in the massif would benefit from future studies combining lithological influences with other factors such as failure mode and runout behaviour. Temporal statistical landslide susceptibility studies account for changes in where landslides occur over time due to changes in feature behaviour and could also be conducted to assess changing climatic conditions and glacial retreat on inter-eruptive landslide susceptibility. This assessment would likely require a smaller range of included landslide forms and larger study area as there would have to be enough temporal variation in landslide events to detect patterns with the feature datasets.

Author Contributions

JPC contributed to the formal analysis, software script development, methodology and writing (original draft) in this paper. SAS contributed to the conceptualization, supervision, resources, project administration, methodology, funding acquisition and writing (review and editing). GWJ contributed to the resources, project administration, methodology, funding acquisition and writing (review and editing).

Acknowledgements

We would like to thank the Líl̓wat Nation and Meager Creek Development Corporation (MCDC) for their great support and assistance in the project. Thanks to A. Tellez, M. Muhammad and B. Coughlan for their hard work assisting in the field. The technical guidance received during the project from T. Millard is deeply appreciated. This project would not have been possible without support and access to the Digital Research Alliance of Canada supercomputing facilities. Funding for this project was generously provided by Mitacs Accelerate grant (#IT29699) supported by MCDC, and the Forest Renewal BC Research Chair in Resource Geoscience and Geotechnics endowment fund.

Data Availability

Data are available upon request.

Copyright Notice

References

Akinci, H. and M. Zeybek (2021). "Comparing classical statistic and machine learning models in landslide susceptibility mapping in Ardanuc (Artvin), Turkey". *Natural Hazards* 108(2), pages 1515–1543. DOI: 10.1007/s11069-021-04743-4.

Aligholi, S., G. R. Lashkaripour, and M. Ghafoori (2017). "Strength/Brittleness Classification of Igneous Intact Rocks Based on Basic Physical and Dynamic Properties". *Rock Mechanics and Rock Engineering* 50(1), pages 45–65. DOI: 10.1007/s00603-016-1106-x.

Amato, G., C. Eisank, D. Castro-Camilo, and L. Lombardo (2019). "Accounting for covariate distributions in slope-unit-based landslide susceptibility models. A case study in the alpine environment". *Engineering Geology* 260. DOI: 10.1016/j.enggeo.2019.105237.

Amit, Y., D. Geman, and K. Wilder (1997). "Joint induction of shape features and tree classifiers". *Pattern Analysis and Machine Intelligence* 19(11), pages 1300–1305. DOI: 10.1109/34.632990.

Anderson, R. G. (1975). "The geology of the volcanics of the Meager Creek map area, southwestern British Columbia". B.Sc. thesis. University of British Columbia.

Andrews, G. D. M., J. K. Russell, S. R. Brown, and R. J. Enkin (2012). "Pleistocene reversal of the Fraser River, British Columbia". *Geology* 40(2), pages 111–114. DOI: 10.1130/G32488.1.

Andrews, G. D. M., J. K. Russell, and M. L. Stewart (2014). "The history and dynamics of a welded pyroclastic dam and its failure". *Bulletin of Volcanology* 76(4), page 811. DOI: 10.1007/s00445-014-0811-0.

Angelbeck, B., C. Springer, J. Jones, G. Williams-Jones, and M. C. Wilson (2024). "Líl̓wat climbers could see the ocean from the peak of Qelqelústen: Evaluating oral traditions with viewshed analyses from the Mount Meager massif prior to its 2360 BP eruption". *American Antiquity*, pages 1–21. DOI: 10.1017/aaq.2024.26.

Barman, J., D. D. L. Soren, and B. Biswas (2023). "Landslide Susceptibility Evaluation and Analysis: A Review on Articles Published During 2000 to 2020". *Monitoring and Managing Multi-hazards: A Multidisciplinary Approach*. Edited by J. Das and S. K. Bhattacharya. Springer International Publishing, pages 211–220. DOI: 10.1007/978-3-031-15377-8_14.

Baumann Engineering (1999). *Meager Creek Geological Hazards and Risk Management [Terrain Features and Surficial Geology Map]*. Technical report. British Columbia Ministry of Forests.

Begét, J. E. and J. Kienle (1992). "Cyclic formation of debris avalanches at Mount St Augustine volcano". *Nature* 356(6371), pages 701–704. DOI: 10.1038/356701a0.

Biecek, P. (2018). "DALEX: Explainers for Complex Predictive Models in R". *Journal of Machine Learning Research* 19(84), pages 1–5.

Bovis, M. J. (1982). "Uphill-facing (antislope) scarps in the Coast Mountains, southwest British Columbia". *GSA Bulletin* 93(8), pages 804–812. DOI: 10.1130/0016-7606(1982)93<804:UASITC>2.0.CO;2.

– (1990). "Rock-slope deformation at Affliction Creek, southern Coast Mountains, British Columbia". *Canadian Journal of Earth Sciences* 27(2), pages 243–254. DOI: 10.1139/e90-024.

Bovis, M. J. and S. G. Evans (1996). "Extensive deformations of rock slopes in southern Coast Mountains, southwest British Columbia, Canada". *Engineering Geology* 44(1), pages 163–182. DOI: 10.1016/S0013-7952(96)00068-3.

Bovis, M. J. and M. Jakob (2000). "The July 29, 1998, debris flow and landslide dam at Capricorn Creek, Mount Meager Volcanic Complex, southern Coast Mountains, British Columbia". *Canadian Journal of Earth Sciences* 37(10), pages 1321–1334. DOI: 10.1139/e00-042.

Box, G. E. P. and P. W. Tidwell (1962). "Transformation of the Independent Variables". *Technometrics* 4(4), pages 531–550. DOI: 10.2307/1266288.

Breiman, L. (1996). "Bagging predictors". *Machine Learning* 24(2), pages 123–140. DOI: 10.1007/BF00058655.

– (1997). *Out-of-bag estimation*. Technical report. University of California, Department of Statistics.

– (2001). "Random Forests". *Machine Learning* 45(1), pages 5–32. DOI: 10.1023/A:1010933404324.

Brenning, A. (2005). "Spatial prediction models for landslide hazards: Review, comparison and evaluation". *Natural Hazards and Earth System Sciences* 5(6), pages 853–862. DOI: 10.5194/nhess-5-853-2005.

Brocklehurst, S. H. and K. X. Whipple (2007). "Response of glacial landscapes to spatial variations in rock uplift rate". *Journal of Geophysical Research: Earth Surface* 112(F2). DOI: 10.1029/2006JF000667.

Budimir, M. E. A., P. M. Atkinson, and H. G. Lewis (2015). "A systematic review of landslide probability mapping using logistic regression". *Landslides* 12(3), pages 419–436. DOI: 10.1007/s10346-014-0550-5.

Burbank, D. W., J. Leland, E. Fielding, R. S. Anderson, N. Brozovic, M. R. Reid, and C. Duncan (1996). "Bedrock incision, rock uplift and threshold hillslopes in the northwestern Himalayas". *Nature* 379(6565), pages 505–510. DOI: 10.1038/379505a0.

Callens, A., D. Morichon, S. Abadie, M. Delpey, and B. Liquet (2020). "Using Random forest and Gradient boosting trees to improve wave forecast at a specific location". *Applied Ocean Research* 104, page 102339. DOI: 10.1016/j.apor.2020.102339.

Camilo, D. C., L. Lombardo, P. M. Mai, J. Dou, and R. Huser (2017). "Handling high predictor dimensionality in slope-unit-based landslide susceptibility models through LASSO-penalized Generalized Linear Model". *Environmental Modelling & Software* 97, pages 145–156. DOI: 10.1016/j.envsoft.2017.08.003.

Carrara, A., M. Cardinali, F. Guzzetti, and P. Reichenbach (1995). "Gis Technology in Mapping Landslide Hazard". *Geographical Information Systems in Assessing Natural Hazards*. Edited by A. Carrara and F. Guzzetti. Springer Netherlands, pages 135–175. DOI: 10.1007/978-94-015-8404-3_8.

Cecchi, E., B. Wyk de Vries, and J.-M. Lavest (2004). "Flank spreading and collapse of weak-cored volcanoes". *Bulletin of Volcanology* 67, pages 72–91. DOI: 10.1007/s00445-004-0369-3.

Chen, C., Z. Shen, Y. Weng, S. You, J. Lin, S. Li, and K. Wang (2023). "Modeling Landslide Susceptibility in Forest-Covered Areas in Lin'an, China, Using Logistical Regression, a Decision Tree, and Random Forests". *Remote Sensing* 15(18). DOI: 10.3390/rs15184378.

Chen, W., X. Li, Y. Wang, G. Chen, and S. Liu (2014). "Forested landslide detection using LiDAR data and the random forest algorithm: A case study of the Three Gorges, China". *Remote Sensing of Environment* 152, pages 291–301. DOI: 10.1016/j.rse.2014.07.004.

Chen, Z., S. E. Grasby, and X. Liu (2021). "Chapter 3—Fracture system analyses of the Mount Meager area". *Garibaldi Geothermal Energy Project - Phase 1 Final Report*. Geoscience BC, pages 34–48.

Chernyshev, I. V., V. Lebedev, S. N. Bubnov, M. M. Arakelyants, and Y. V. Gol'tsman (2002). "Isotopic geochronology of Quaternary volcanic eruptions in the Greater Caucasus". *Geochemistry International* 40, pages 1042–1055.

Church, M. and M. Ryder (2010). "Physiography of British Columbia Chapter 2". *Compendium of forest hydrology and geomorphology in British Columbia*. Edited by R. G. Pike, T. E. Redding, R. D. Moore, R. D. Winker, and K. D. Bladon. Victoria, B.C.: B.C. Ministry of Forests et al.

Clague, J. J., S. G. Evans, V. N. Rampton, and G. J. Woodsworth (1995). "Improved age estimates for the White River and Bridge River tephras, western Canada". *Canadian Journal of Earth Sciences* 32(8), pages 1172–1179. DOI: 10.1139/e95-096.

Clague, J. J., J. R. Harper, R. J. Hebda, and D. E. Howes (1982). "Late Quaternary sea levels and crustal movements, coastal British Columbia". *Canadian Journal of Earth Sciences* 19(3), pages 597–618. DOI: 10.1139/e82-048.

Clague, J. J. and T. S. James (2002). "History and isostatic effects of the last ice sheet in southern British Columbia". *Quaternary Science Reviews* 21(1), pages 71–87. DOI: 10.1016/S0277-3791(01)00070-1.

Clague, J. J. and B. Ward (2011). "Chapter 44—Pleistocene Glaciation of British Columbia". *Developments in Quaternary Sciences*. Edited by J. Ehlers, P. L. Gibbard, and P. D. Hughes. Volume 15. Elsevier, pages 563–573. DOI: 10.1016/B978-0-444-53447-7.00044-1.

Crozier, M. J. and T. Glade (2005). "Landslide Hazard and Risk: Issues, Concepts and Approach". *Landslide Hazard and Risk*. Edited by T. Glade, M. Anderson, and M. J. Crozier. John Wiley & Sons, Ltd, pages 1–40. DOI: 10.1002/9780470012659.ch1.

Cruden, D. M. (1991). "A simple definition of a landslide". *Bulletin of the International Association of Engineering Geology - Bulletin de l'Association Internationale de Géologie de l'Ingénieur* 43(1), pages 27–29. DOI: 10.1007/BF02590167.

Cruden, D. M. and D. J. Varnes (1996). "Chapter 3: Landslide Types and Processes". *Landslides: Investigation and mitigation*. Volume 247. Special Report National Research Council Transportation Research Board, pages 36–75.

Delcamp, A., G. Roberti, and B. van Wyk de Vries (2016). "Water in volcanoes: Evolution, storage and rapid release during landslides". *Bulletin of Volcanology* 78(12). DOI: 10.1007/s00445-016-1082-8.

Del Potro, R. and M. Hürlimann (2008). "Geotechnical classification and characterisation of materials for stability analyses of large volcanic slopes". *Engineering Geology* 98(1), pages 1–17. DOI: 10.1016/j.enggeo.2007.11.007.

– (2009). "The decrease in the shear strength of volcanic materials with argillic hydrothermal alteration, insights from the summit region of Teide stratovolcano, Tenerife". *Engineering Geology* 104(1), pages 135–143. DOI: 10.1016/j.enggeo.2008.09.005.

Denton, G. H. and R. L. Armstrong (1969). "Miocene-Pliocene glaciations in southern Alaska". *American Journal of Science* 267(10), pages 1121–1142. DOI: 10.2475/ajs.267.10.1121.

Detterman, R. L. and J. K. Hartsock (1966). *Geology of the Iniskin-Tuxedni region, Alaska*. Technical report. United States Government, page 78. DOI: 10.3133/pp512.

Ehlers, T. A., K. A. Farley, M. E. Rusmore, and G. J. Woodsworth (2006). "Apatite (U-Th)/He signal of large-magnitude accelerated glacial erosion, southwest British Columbia". *Geology* 34(9), pages 765–768. DOI: 10.1130/G22507.1.

Entwisle, D. C., P. R. N. Hobbs, L. D. Jones, D. Gunn, and M. G. Raines (2005). "The Relationships between Effective Porosity, Uniaxial Compressive Strength and Sonic Velocity of Intact Borrowdale Volcanic Group Core Samples from Sellafield". *Geotechnical & Geological Engineering* 23(6), pages 793–809. DOI: 10.1007/s10706-004-2143-x.

Evans, S. G. (1987). "A rock avalanche from the peak of Mount Meager, British Columbia". *Geological Survey of Canada* 87-1A, pages 929–933. DOI: 10.4095/122564.

Evans, S. G., O. V. Tutubalina, V. N. Drobyshev, S. S. Chernomorets, S. McDougall, D. A. Petrakov, and O. Hungr (2009). "Catastrophic detachment and high-velocity long-runout flow of Kolka Glacier, Caucasus Mountains, Russia in 2002". *Geomorphology* 105(3), pages 314–321. DOI: 10.1016/j.geomorph.2008.10.008.

Farley, K. A., M. E. Rusmore, and S. W. Bogue (2001). "Post–10 Ma uplift and exhumation of the northern Coast Mountains, British Columbia". *Geology* 29(2), pages 99–102. DOI: 10.1130/0091-7613(2001)029<0099:PMUAEO>2.0.CO;2.

Farquharson, J., M. J. Heap, N. R. Varley, P. Baud, and T. Reuschlé (2015). "Permeability and porosity relationships of edifice-forming andesites: A combined field and laboratory study". *Journal of Volcanology and Geothermal Research* 297, pages 52–68. DOI: 10.1016/j.jvolgeores.2015.03.016.

Fell, R. (1994). "Landslide risk assessment and acceptable risk". *Canadian Geotechnical Journal* 31(2), pages 261–272. DOI: 10.1139/t94-031.

Fleuchaus, P., P. Blum, M. Wilde, B. Terhorst, and C. Butscher (2021). "Retrospective evaluation of landslide susceptibility maps and review of validation practice". *Environmental Earth Sciences* 80(15), page 485. DOI: 10.1007/s12665-021-09770-9.

Friedman, J. H. (2001). "Greedy function approximation: A gradient boosting machine". *The Annals of Statistics* 29(5), pages 1189–1232. DOI: 10.1214/aos/1013203451.

Friele, P. A. (2012). "Volcanic Landslide Risk Management, Lillooet River Valley, BC: Start of north and south FSRs to Meager Confluence, Meager Creek and Upper Lillooet River". PhD thesis. University of British Columbia.

Friele, P. A. and J. J. Clague (2004). "Large Holocene landslides from Pylon Peak, southwestern British Columbia". *Canadian Journal of Earth Sciences* 41(2), pages 165–182. DOI: 10.1139/e03-089.

Friele, P. A., J. J. Clague, K. Simpson, and M. Stasiuk (2005). "Impact of a Quaternary volcano on Holocene sedimentation in Lillooet River valley, British Columbia". *Sedimentary Geology* 176(3), pages 305–322. DOI: 10.1016/j.sedgeo.2005.01.011.

Friele, P. A., M. Jakob, and J. Clague (2008). "Hazard and risk from large landslides from Mount Meager volcano, British Columbia, Canada". *Georisk: Assessment and Management of Risk for Engineered Systems and Geohazards* 2(1), pages 48–64. DOI: 10.1080/17499510801958711.

Frolova, J. V., M. S. Chernov, S. N. Rychagov, V. M. Ladygin, V. N. Sokolov, and R. A. Kuznetsov (2021). "The influence of hydrothermal argillization on the physical and mechanical properties of tuffaceous rocks: A case study from the Upper Pauzhetsky thermal field, Kamchatka". *Bulletin of Engineering Geology and the Environment* 80(2), pages 1635–1651. DOI: 10.1007/s10064-020-02007-2.

Gehrels, G., M. Rusmore, G. Woodsworth, M. Crawford, C. Andronicos, L. Hollister, J. Patchett, M. Ducea, R. Butler, K. Klepeis, C. Davidson, R. Friedman, J. Haggart, B. Mahoney, W. Crawford, D. Pearson, and J. Girardi (2009). "U-Th-Pb geochronology of the Coast Mountains batholith in north-coastal British Columbia: Constraints on age and tectonic evolution". *GSA Bulletin* 121(9–10), pages 1341–1361. DOI: 10.1130/B26404.1.

Gini, C. (1912). *Variabilità e mutabilità*. Edited by E. Pizetti and T. Salvemini. Reprinted in Memorie di metodologica statistica.

Girina, O. A. (2013). "Chronology of Bezymianny Volcano activity, 1956–2010". *Journal of Volcanology and Geothermal Research* 263, pages 22–41. DOI: 10.1016/j.jvolgeores.2013.05.002.

Gorshkov, G. S. (1959). "Gigantic eruption of the volcano Bezymianny". *Bulletin Volcanologique* 20, pages 77–109.

Grasby, S. E., S. M. Ansari, A. Calahorrano-DiPatre, Z. Chen, J. A. Craven, J. Dettmer, H. Gilbert, C. Hanneson, M. Harris, J. K. Russell, R. O. Salvage, G. Savard, V. Tschirhart, M. J. Unsworth, N. Vigouroux-Caillibot, G. Williams-Jones, A. R. Williamson, R. W. Barendregt, A. Borch, and J. Liu (2021). "Garibaldi Geothermal Energy Project—Phase 1 Final Report".

Greenwell, B. M., B. C. Boehmke, and A. J. McCarthy (2018). "A Simple and Effective Model-Based Variable Importance Measure". *arXiv*. DOI: 10.48550/arXiv.1805.04755.

Guthrie, R., P. Friele, K. Allstadt, N. Roberts, S. Evans, K. Delaney, D. Roche, J. Clague, and M. Jakob (2012). "The 6 August 2010 Mount Meager rock slide-debris flow, Coast Mountains, British Columbia: Characteristics, dynamics, and implications for hazard and risk assessment". *Natural Hazards and Earth System Sciences* 12, pages 1277–1294. DOI: 10.5194/nhess-12-1277-2012.

Guzzetti, F., A. Carrara, M. Cardinali, and P. Reichenbach (1999). "Landslide hazard evaluation: A review of current techniques and their application in a multi-scale study, Central Italy". *Geomorphology* 31(1), pages 181–216. DOI: 10.1016/S0169-555X(99)00078-1.

Guzzetti, F., P. Reichenbach, F. Ardizzone, M. Cardinali, and M. Galli (2006). "Estimating the quality of landslide susceptibility models". *Geomorphology* 81(1–2), pages 166–184. DOI: 10.1016/j.geomorph.2006.04.007.

Hammond, P. E. (1979). "A tectonic model for the evolution of the Cascade Range". *Cenozoic Paleogeography of the Western United States*, pages 219–237.

Hanneson, C. and M. J. Unsworth (2023). "Magnetotelluric imaging of the magmatic and geothermal systems beneath Mount Meager, southwestern Canada". *Canadian Journal of Earth Sciences* 60(10), pages 1385–1403. DOI: 10.1139/cjes-2022-0136.

Harris, M. and J. K. Russell (2021). "Chapter 2—Bedrock Mapping Results for the Mount Meager Geothermal Research Initiative". *Garibaldi Geothermal Energy Project—Phase 1 Final Report*. Geoscience BC, pages 34–48.

Harris, M., J. K. Russell, M. Muhammad, and G. Williams-Jones (2021). *Mount Meager Volcanic Complex, Garibaldi Volcanic Belt, Canada: Expanded Bedrock Map including Cracked Mountain, North Lillooet Ridge, and West Mount Meager (Open File 8881)*. Technical report. Geological Survey of Canada.

Harris, M., J. K. Russell, A. Wilson, and B. Jicha (2023). "A 500 ka record of volcanism and paleoenvironment in the northern Garibaldi Volcanic Belt, British Columbia". *Canadian Journal of Earth Sciences* 60(4), pages 401–421. DOI: 10.1139/cjes-2022-0101.

He, Q., M. Wang, and K. Liu (2021). "Rapidly assessing earthquake-induced landslide susceptibility on a global scale using random forest". *Geomorphology* 391, page 107889. DOI: 10.1016/j.geomorph.2021.107889.

Heap, M. J., D. M. Gravley, B. M. Kennedy, H. A. Gilg, E. Bertolett, and S. L. Barker (2020). "Quantifying the role of hydrothermal alteration in creating geothermal and epithermal mineral resources: The Ohakuri ignimbrite (Taupō Volcanic Zone, New Zealand)". *Journal of Volcanology and Geothermal Research* 390, page 106703. DOI: 10.1016/j.jvolgeores.2019.106703.

Heap, M. J. and M. E. Violay (2021). "The mechanical behaviour and failure modes of volcanic rocks: a review". *Bulletin of Volcanology* 83(5). DOI: 10.1007/s00445-021-01447-2.

Hetherington, R. (2014). "Slope Stability Analysis of Mount Meager, south-western British Columbia, Canada". Michigan Technological University.

Hewitt, K. (1998). "Catastrophic landslides and their effects on the Upper Indus streams, Karakoram Himalaya, northern Pakistan". *Geomorphology* 26(1), pages 47–80. DOI: 10.1016/S0169-555X(98)00051-8.

Hickson, C. J., J. K. Russell, and M. V. Stasiuk (1999). "Volcanology of the 2350 B.P. Eruption of Mount Meager Volcanic Complex, British Columbia, Canada: Implications for Hazards from Eruptions in Topographically Complex Terrain". *Bulletin of Volcanology* 60(7), pages 489–507. DOI: 10.1007/s004450050247.

Hickson, C. J. and J. G. Souther (1984). "Late Cenozoic volcanic rocks of the Clearwater – Wells Gray area, British Columbia". *Canadian Journal of Earth Sciences* 21(3), pages 267–277. DOI: 10.1139/e84-029.

Hildreth, W. (2007). *Quaternary magmatism in the Cascades—Geologic perspectives*. U.S. Geological Survey, pages 44–56. DOI: 10.3133/pp1744.

Holm, K., M. Bovis, and M. Jakob (2004). "The landslide response of alpine basins to post-Little Ice Age glacial thinning and retreat in southwestern British Columbia". *Geomorphology* 57(3), pages 201–216. DOI: 10.1016/S0169-555X(03)00103-X.

Hormozzade Ghalati, F., J. A. Craven, D. Motazedian, S. E. Grasby, E. Roots, V. Tschirhart, Z. Chen, and X. Liu (2023). "Analysis of Fluid Flow Pathways in the Mount Meager Volcanic Complex, Southwestern Canada, Utilizing AMT and Petrophysical Data". *Geochemistry, Geophysics, Geosystems* 24(3), e2022GC010519. DOI: 10.1029/2022GC010519.

Hormozzade Ghalati, F., J. A. Craven, D. Motazedian, S. E. Grasby, and V. Tschirhart (2022). "Modeling a fractured geothermal reservoir using 3-D AMT data inversion: Insights from Garibaldi Volcanic Belt, British Columbia, Canada". *Geothermics* 105, page 102528. DOI: 10.1016/j.geothermics.2022.102528.

Horton, P., M. Jaboyedoff, B. Rudaz, and M. Zimmermann (2013). "Flow-R, a model for susceptibility mapping of debris flows and other gravitational hazards at a regional scale". *Natural Hazards and Earth System Sciences* 13(4), pages 869–885. DOI: 10.5194/nhess-13-869-2013.

Hosmer, D. W. and S. Lemeshow (2000). "Assessing the Fit of the Model". *Applied Logistic Regression*. Edited by W. A. Shewhart and S. S. Wilks. John Wiley & Sons, Ltd, pages 143–202. ISBN: 9780471722144. DOI: 10.1002/0471722146.ch5.

Hovius, N., C. P. Stark, and P. A. Allen (1997). "Sediment flux from a mountain belt derived by landslide mapping". *Geology* 25(3), pages 231–234. DOI: 10.1130/0091-7613(1997)025<0231:SFFAMB>2.3.CO;2.

Huggel, C., J. Caplan-Auerbach, C. F. Waythomas, and R. L. Wessels (2007). "Monitoring and modeling ice-rock avalanches from ice-capped volcanoes: A case study of frequent large avalanches on Iliamna Volcano, Alaska". *Journal of Volcanology and Geothermal Research* 168(1), pages 114–136. DOI: 10.1016/j.jvolgeores.2007.08.009.

Huggel, C., J. Caplan-Auerbach, and R. Wessels (2008). "Recent Extreme Avalanches: Triggered by Climate Change?" *Eos, Transactions American Geophysical Union* 89(47), pages 469–470. DOI: 10.1029/2008EO470001.

Hungr, O. and S. G. Evans (2004). "Entrainment of debris in rock avalanches: An analysis of a long run-out mechanism". *Geological Society of America Bulletin* 116(9), page 1240. DOI: 10.1130/B25362.1.

Hungr, O., S. Leroueil, and L. Picarelli (2014). "The Varnes classification of landslide types, an update". *Landslides* 11(2), pages 167–194. DOI: 10.1007/s10346-013-0436-y.

Hürlimann, M., A. Ledesma, and J. Martı (2001). "Characterisation of a volcanic residual soil and its implications for large landslide phenomena: Application to Tenerife, Canary Islands". *Engineering Geology* 59(1), pages 115–132. DOI: 10.1016/S0013-7952(00)00069-7.

James, T. S., J. J. Clague, K. Wang, and I. Hutchinson (2000). "Postglacial rebound at the northern Cascadia subduction zone". *Quaternary Science Reviews* 19(14), pages 1527–1541. DOI: 10.1016/S0277-3791(00)00076-7.

Jamieson, G. R. (1981). "A preliminary study of the regional groundwater flow in the Meager Mountain geothermal area, British Columbia". PhD thesis. University of British Columbia. DOI: 10.14288/1.0052666.

Jamieson, G. R. and R. A. Freeze (1982). "Determining Hydraulic Conductivity Distributions in a Mountainous Area Using Mathematical Modeling". *Groundwater* 20(2), pages 168–177. DOI: 10.1111/j.1745-6584.1982.tb02745.x.

Jennings, C., J. Aber, G. Balco, R. Barendregt, P. R. Bierman, C. Rovey, M. Roy, H. Thorleifson, and J. A. Mason (2007). "GLACIATIONS | Mid-Quaternary in North America". *Encyclopedia of Quaternary Science*. Elsevier, pages 180–186. DOI: 10.1016/B978-0-444-53643-3.00124-2.

Jessop, A. M., M. M. Ghomshei, and M. J. Drury (1991). "Geothermal energy in Canada". *Geothermics* 20(5), pages 369–385. DOI: 10.1016/0375-6505(91)90027-S.

Jones, J. (2011). "Lil'wat Landscapes". *The Midden* 43(1), Article 1.

Jordan, R. P. (1995). "Debris flows in the southern Coast Mountains, British Columbia : dynamic behaviour and physical properties". PhD thesis. University of British Columbia. DOI: 10.14288/1.0088849.

Kariya, Y., G. Sato, and M. Arai (2006). "Large-Scale Landslides in Rapidly Uplifted and Extremely Snowy Mountains in the Northern Japanese Alps". *AGU Fall Meeting Abstracts*.

Kelman, M. C. and A. M. Wilson (2024). "Assessing the relative threats from Canadian volcanoes". *Canadian Journal of Earth Sciences* 61(3), pages 408–430. DOI: 10.1139/cjes-2023-0074.

Kerr, R. A. (1984). "Landslides from Volcanoes Seen as Common". *Science* 224(4646), pages 275–276.

Klaasen, S., P. Paitz, N. Lindner, J. Dettmer, and A. Fichtner (2021). "Distributed Acoustic Sensing in Volcano-Glacial Environments—Mount Meager, British Columbia". *Journal of Geophysical Research: Solid Earth* 126(11). DOI: 10.1029/2021jb022358.

Lewis, T. J., A. S. Judge, and J. G. Souther (1978). "Possible geothermal resources in the Coast Plutonic Complex of southern British Columbia, Canada". *Pure and Applied Geophysics* 117(1), pages 172–179. DOI: 10.1007/BF00879744.

Liang, Z., C. Wang, D. Ma, and K. U. J. Khan (2021). "Exploring the potential relationship between the occurrence of debris flow and landslides". *Natural Hazards and Earth System Sciences* 21(4), pages 1247–1262. DOI: 10.5194/nhess-21-1247-2021.

Lipman, P. W. (1981). "Building of the north flank before the May 18 eruption-Geodetic data". *US Geological Survey Professional Paper* 1250, pages 143–155.

Lombardo, L. and P. M. Mai (2018). "Presenting logistic regression-based landslide susceptibility results". *Engineering Geology* 244, pages 14–24. DOI: 10.1016/j.enggeo.2018.07.019.

López, D. L. and S. N. Williams (1993). "Catastrophic Volcanic Collapse: Relation to Hydrothermal Processes". *Science* 260(5115), pages 1794–1796. DOI: 10.1126/science.260.5115.1794.

Louppe, G. (2015). "Understanding Random Forests: From Theory to Practice". *arXiv*. DOI: 10.48550/ARXIV.1407.7502.

Lu, L. and M. G. Bostock (2022). "Deep long-period earthquakes near Mount Meager, British Columbia". *Canadian Journal of Earth Sciences* 59(7), pages 407–417. DOI: 10.1139/cjes-2021-0103.

Malawani, M. N., F. Lavigne, K. Kelfoun, P. Lahitte, D. S. Hadmoko, C. Gomez, P. Wassmer, S. Syamsuddin, and A. Faral (2024). "Large debris avalanche and associated eruptive event at Samalas volcano, Lombok, Indonesia". *Bulletin of Volcanology* 86(3), page 24. DOI: 10.1007/s00445-024-01727-7.

Mandrekar, J. N. (2010). "Receiver Operating Characteristic Curve in Diagnostic Test Assessment". *Journal of Thoracic Oncology* 5(9), pages 1315–1316. DOI: 10.1097/jto.0b013e3181ec173d.

Mathews, W. H., J. G. Fyles, and H. W. Nasmith (1970). "Postglacial crustal movements in southwestern British Columbia and adjacent Washington state". *Canadian Journal of Earth Sciences* 7(2), pages 690–702. DOI: 10.1139/e70-068.

McGuire, B. (2003). "Volcano instability and lateral collapse". *Revista* 1, pages 33–45.

Merghadi, A., A. P. Yunus, J. Dou, J. Whiteley, B. ThaiPham, D. T. Bui, R. Avtar, and B. Abderrahmane (2020). "Machine learning methods for landslide susceptibility studies: A comparative overview of algorithm performance". *Earth-Science Reviews* 207, page 103225. DOI: 10.1016/j.earscirev.2020.103225.

Millard, T., T. P. Rollerson, and B. Thomson (2002). *Post-logging landslide rates in the Cascade Mountains, southwestern British Columbia*. Forest Research Technical Report TR-023; Geomorphology, p. 21. [Research Section], Vancouver Forest Region.

Mitchell, A. D., S. D. McDougall, and J. B. Aaron (2018). "Benchmarking exercise: Dan3D with objective calibration methods". *Proceedings of the second JTC1 workshop, triggering and propagation of rapid flow-like landslides, Hong Kong*, pages 3–5.

Mitchell, A. D., S. D. McDougall, J. B. Aaron, and M.-A. Brideau (2020). "Rock Avalanche-Generated Sediment Mass Flows: Definitions and Hazard". *Frontiers in Earth Science* 8. DOI: 10.3389/feart.2020.543937.

Mitchell, A. D., S. D. McDougall, N. Nolde, M.-A. Brideau, J. Whittall, and J. B. Aaron (2019). "Rock avalanche runout prediction using stochastic analysis of a regional dataset". *Landslides* 17(4), pages 777–792. DOI: 10.1007/s10346-019-01331-3.

Mokievsky-Zubok, O. (1977). "Glacier-caused slide near Pylon Peak, British Columbia". *Canadian Journal of Earth Sciences* 14(11), pages 2657–2662. DOI: 10.1139/e77-230.

Moore, J. G. (1981). "Topographic and structural change, March-July 1980-photogrammetric data". *US Geol. Surv. Prof. Paper* 1250, pages 123–134.

Morison, C. A. G. and C. J. Hickson (2023). "Mount Garibaldi: hazard potential from a long-dormant volcanic system in the Pacific Northwest". *Canadian Journal of Earth Sciences* 60(5), pages 464–484. DOI: 10.1139/cjes-2022-0067.

Mueller, S., O. Melnik, O. Spieler, B. Scheu, and D. B. Dingwell (2005). "Permeability and degassing of dome lavas undergoing rapid decompression: An experimental determination". *Bulletin of Volcanology* 67(6), pages 526–538. DOI: 10.1007/s00445-004-0392-4.

Muhammad, M., G. Williams-Jones, and R. W. Barendregt (2024). "Structural geology of the Mount Meager Volcanic Complex, BC, Canada: implications for geothermal energy and geohazards". *Canadian Journal of Earth Sciences* 61(2), pages 158–186. DOI: 10.1139/cjes-2023-0077.

Muhammad, M., G. Williams-Jones, D. Stead, R. Tortini, G. Falorni, and D. Donati (2022). "Applications of Image-Based Computer Vision for Remote Surveillance of Slope Instability". *Frontiers in Earth Science* 10. DOI: 10.3389/feart.2022.909078.

Natural Resources Canada (2019). *2015 Land Cover of Canada—Open Government Portal*. URL: https://open.canada.ca%20/data/en/dataset/4e615eae-b90c-420b-adee-2ca35896caf6 (visited on 07/31/2022).

NSBG (1985). *Multielement geochemistry of the Meager creek geothermal system (gt22)*. Technical report 122. Earth Sciences Laboratory - University of Utah Research Institute.

Parrish, R. R. (1983). "Cenozoic thermal evolution and tectonics of the Coast Mountains of British Columbia: 1. Fission track dating, apparent uplift rates, and patterns of uplift". *Tectonics* 2(6), pages 601–631. DOI: 10.1029/TC002i006p00601.

Petschko, H., A. Brenning, R. Bell, J. Goetz, and T. Glade (2014). "Assessing the quality of landslide susceptibility maps – case study Lower Austria". *Natural Hazards and Earth System Sciences* 14(1), pages 95–118. DOI: 10.5194/nhess-14-95-2014.

Planet Labs PBC (2018). *Planet Application Program Interface: In Space for Life on Earth*. URL: https://api.planet.com (visited on 07/31/2024).

Probst, P., M. N. Wright, and A.-L. Boulesteix (2019). "Hyperparameters and tuning strategies for random forest". *WIREs Data Mining and Knowledge Discovery* 9(3). DOI: 10.1002/widm.1301.

Read (1977). *Meager Creek volcanic complex, southwestern British Columbia*. 77th-1A: 277-281st ed. [Map].

Read, P. B. (1990). "Mount Meager Complex, Garibaldi Belt, Southwestern British Columbia". *Geoscience Canada* 17(3), pages 167–170.

Reichenbach, P., M. Rossi, B. D. Malamud, M. Mihir, and F. Guzzetti (2018). "A review of statistically-based landslide susceptibility models". *Earth-Science Reviews* 180, pages 60–91. DOI: 10.1016/j.earscirev.2018.03.001.

Reiners, P. W., T. A. Ehlers, J. I. Garver, S. G. Mitchell, D. R. Montgomery, J. A. Vance, and S. Nicolescu (2002). "Late Miocene exhumation and uplift of the Washington Cascade Range". *Geology* 30(9), page 767. DOI: 10.1130/0091-7613(2002)030<0767:lmeauo>2.0.co;2.

Roberti, G. (2018). "Mount Meager, a glaciated volcano in a changing cryosphere: Hazards and risk challenges". PhD thesis. Simon Fraser University and Université Clermont Auvergne.

Roberti, G., P. Friele, B. van Wyk de Vries, B. Ward, J. J. Clague, L. Perotti, and M. Giardino (2017). "Rheological evolution of the Mount Meager 2010 debris avalanche, southwestern British Columbia". *Geosphere* 13(2), pages 369–390. DOI: 10.1130/ges01389.1.

Roverato, M., P. Larrea, I. Casado, M. Mulas, G. Béjar, and L. Bowman (2018). "Characterization of the Cubilche debris avalanche deposit, a controversial case from the northern Andes, Ecuador". *Journal of Volcanology and Geothermal Research* 360, pages 22–35. DOI: 10.1016/j.jvolgeores.2018.07.006.

Russell, J. K., B. R. Edwards, G. Williams-Jones, and C. J. Hickson (2023). "Pleistocene to Holocene volcanism in the Canadian Cordillera". *Canadian Journal of Earth Sciences* 60(10), pages 1443–1466. DOI: 10.1139/cjes-2023-0065.

Russell, J. K., M. Stewart, A. Wilson, and G. Williams-Jones (2021). "Eruption of Mount Meager, British Columbia, during the early Fraser glaciation". *Canadian Journal of Earth Sciences* 58(10), pages 1146–1154. DOI: 10.1139/cjes-2021-0023.

Ryder, J. M. and B. Thomson (1986). "Neoglaciation in the southern Coast Mountains of British Columbia: chronology prior to the late Neoglacial maximum". *Canadian Journal of Earth Sciences* 23(3), pages 273–287. DOI: 10.1139/e86-031.

Sahin, E. K., I. Colkesen, and T. Kavzoglu (2018). "A comparative assessment of canonical correlation forest, random forest, rotation forest and logistic regression methods for landslide susceptibility mapping". *Geocarto International* 35(4), pages 341–363. DOI: 10.1080/10106049.2018.1516248.

Scornet, E. (2020). "Trees, forests, and impurity-based variable importance". *arXiv*. DOI: 10.48550/ARXIV.2001.04295.

Sekiya, S. (1889). "The eruption of Bandai-san." *Journal of the College of Science, Imperial University Tokyo* 3, pages 91–172.

Shea, T. and B. Van Wyk de Vries (2010). "Collapsing volcanoes: the sleeping giants' threat". *Geology Today* 26(2), pages 72–77. DOI: 10.1111/j.1365-2451.2010.00750.x.

Shevchenko, A. V., V. N. Dvigalo, T. R. Walter, R. Mania, F. Maccaferri, I. Y. Svirid, A. B. Belousov, and M. G. Belousova (2020). "The rebirth and evolution of Bezymianny volcano, Kamchatka after the 1956 sector collapse". *Communications Earth & Environment* 1(1). DOI: 10.1038/s43247-020-00014-5.

Shuster, D. L., T. A. Ehlers, M. E. Rusmoren, and K. A. Farley (2005). "Rapid Glacial Erosion at 1.8 Ma Revealed by ^{4}He/^{3}He Thermochronometry". *Science* 310(5754), pages 1668–1670. DOI: 10.1126/science.1118519.

Siebert, L. (1984). "Large volcanic debris avalanches: Characteristics of source areas, deposits, and associated eruptions". *Journal of Volcanology and Geothermal Research* 22(3–4), pages 163–197. DOI: 10.1016/0377-0273(84)90002-7.

Siebert, L. and M. E. Reid (2023). "Lateral edifice collapse and volcanic debris avalanches: a post-1980 Mount St. Helens perspective". *Bulletin of Volcanology* 85(11). DOI: 10.1007/s00445-023-01662-z.

Simpson, K. A., M. Stasiuk, K. Shimamura, J. J. Clague, and P. Friele (2006). "Evidence for catastrophic volcanic debris flows in Pemberton Valley, British Columbia". *Canadian Journal of Earth Sciences* 43(6), pages 679–689. DOI: 10.1139/e06-026.

Souther, J. G. and D. T. A. Symons (1974). *Stratigraphy and paleomagnetism of Mount Edziza volcanic complex, northwest British Columbia*. DOI: 10.4095/102538.

Stewart, M. L., J. K. Russell, and C. J. Hickson (2008). *Geology, Pebble Creek Formation, British Columbia*. Geological Survey of Canada. DOI: 10.4095/225582. [Map].

– (2003). "Discrimination of hot versus cold avalanche deposits: Implications for hazard assessment at Mount Meager, B.C." *Natural Hazards and Earth System Sciences* 3(6), pages 713–724. DOI: 10.5194/nhess-3-713-2003.

Stumpf, A. and N. Kerle (2011). "Object-oriented mapping of landslides using Random Forests". *Remote Sensing of Environment* 115(10), pages 2564–2577. DOI: 10.1016/j.rse.2011.05.013.

Sun, D., J. Xu, H. Wen, and D. Wang (2021). "Assessment of landslide susceptibility mapping based on Bayesian hyperparameter optimization: A comparison between logistic regression and random forest". *Engineering Geology* 281, page 105972. DOI: 10.1016/j.enggeo.2020.105972.

Thorkelson, D. J., J. K. Madsen, and C. L. Sluggett (2011). "Mantle flow through the Northern Cordilleran slab window revealed by volcanic geochemistry". *Geology* 39(3), pages 267–270. DOI: 10.1130/g31522.1.

Tibaldi, A., A. M. F. A. Lagmay, and V. V. Ponomareva (2005). "Effects of basement structural and stratigraphic heritages on volcano behaviour and implications for human activities (the UNESCO/IUGS/IGCP project 455)". *Episodes* 28(3), pages 158–170. DOI: 10.18814/epiiugs/2005/v28i3/002.

Tibshirani, R. (1996). "Regression Shrinkage and Selection via the Lasso". *Journal of the Royal Statistical Society* 58(1), pages 267–288.

Tielidze, L. G., R. M. Kumladze, R. D. Wheate, and M. Gamkrelidze (2019). "The Devdoraki Glacier Catastrophes, Georgian Caucasus". *Hungarian Geographical Bulletin*, pages 21–35. DOI: 10.15201/hungeobull.68.1.2.

Toney, L., D. Fee, K. Allstadt, M. Haney, and R. Matoza (2021). "Reconstructing the dynamics of the highly-similar May 2016 and June 2019 Iliamna Volcano, Alaska ice–rock avalanches from seismoacoustic data". *Earth Surface Dynamics* 9, pages 271–293. DOI: 10.5194/esurf-2020-47.

Unnsteinsson, T., G. E. Flowers, and G. Williams-Jones (2024). "Formation and persistence of glaciovolcanic voids explored with analytical and numerical models". *Journal of Glaciology*, pages 1–15. DOI: 10.1017/jog.2024.8.

Vallier, T. L., D. W. Scholl, M. A. Fisher, T. R. Bruns, F. H. Wilson, R. von Huene, and A. J. Stevenson (1994). "Geologic framework of the Aleutian arc, Alaska". *The Geology of Alaska*. Edited by G. Plafker and H. C. Berg. The Geological Society of America, pages 433–484.

Van der Kooij, M. and A. Lambert (2002). "Results of processing and analysis of large volumes of repeat-pass InSAR data of Vancouver and Mount Meager (B.C.)" *IEEE International Geoscience and Remote Sensing Symposium*. Volume 2. IGARSS-02. IEEE, pages 1228–1230. DOI: 10.1109/igarss.2002.1025897.

Van Westen, C. J., N. Rengers, and R. Soeters (2003). "Use of geomorphological information in indirect landslide susceptibility assessment". *Natural hazards* 30, pages 399–419. DOI: 10.1023/B:NHAZ.0000007097.42735.9e.

Van Wyk de Vries, B. and P. W. Francis (1997). "Catastrophic collapse at stratovolcanoes induced by gradual volcano spreading". *Nature* 387(6631), pages 387–390. DOI: 10.1038/387387a0.

Van Wyk de Vries, B., S. Self, P. Francis, and L. Keszthelyi (2001). "A gravitational spreading origin for the Socompa debris avalanche". *Journal of Volcanology and Geothermal Research* 105(3), pages 225–247. DOI: 10.1016/s0377-0273(00)00252-3.

Van Wyk de Vries, B. and T. Davies (2015). "Landslides, Debris Avalanches, and Volcanic Gravitational Deformation". *The Encyclopedia of Volcanoes*. Edited by H. Sigurdsson. Elsevier, pages 665–685. ISBN: 9780123859389. DOI: 10.1016/b978-0-12-385938-9.00038-9.

Varnes, D. J. (1978). "Slope movement types and processes". *National Academy of Sciences Special report* 176, pages 11–33.

Voight, B. and D. Elsworth (1997). "Failure of volcano slopes". *Géotechnique* 47(1), pages 1–31. DOI: 10.1680/geot.1997.47.1.1.

Wang, W., Z. He, Z. Han, Y. Li, J. Dou, and J. Huang (2020). "Mapping the susceptibility to landslides based on the deep belief network: a case study in Sichuan Province, China". *Natural Hazards* 103(3), pages 3239–3261. DOI: 10.1007/s11069-020-04128-z.

Warwick, R., G. Williams-Jones, M. Kelman, and J. Witter (2022). "A scenario-based volcanic hazard assessment for the Mount Meager Volcanic Complex, British Columbia". *Journal of Applied Volcanology* 11(1). DOI: 10.1186/s13617-022-00114-1.

Watt, S. F. L., D. M. Pyle, J. A. Naranjo, and T. A. Mather (2009). "Landslide and tsunami hazard at Yate volcano, Chile as an example of edifice destruction on strike-slip fault zones". *Bulletin of Volcanology* 71(5), pages 559–574. DOI: 10.1007/s00445-008-0242-x.

Waythomas, C. F. (2012). "Landslides at stratovolcanoes initiated by volcanic unrest". *Landslides*. Cambridge University Press, pages 37–49. DOI: 10.1017/cbo9780511740367.005.

Waythomas, C. F. and T. P. Miller (1999). "Preliminary volcano-hazard assessment for Iliamna Volcano, Alaska". *US Geological Survey Open-File Report* 99-373. DOI: 10.3133/ofr99373.

Werner, C., J. A. Power, P. J. Kelly, S. Prejean, and C. Kern (2022). "Characterizing unrest: A retrospective look at 20 years of gas emissions and seismicity at Iliamna Volcano, Alaska". *Journal of Volcanology and Geothermal Research* 422, page 107448. DOI: 10.1016/j.jvolgeores.2021.107448.

Wilson, A. M. and J. K. Russell (2019). "Quaternary glaciovolcanism in the Canadian Cascade volcanic arc—Paleoenvironmental implications". *Field Volcanology: A Tribute to the Distinguished Career of Don Swanson*. Edited by M. P. Poland, M. O. Garcia, V. E. Camp, and A. Grunder. Volume 538. Geological Society of America, pages 133–157. ISBN: 9780813795386. DOI: 10.1130/2018.2538(06).

Wilson, M. C., B. Angelbeck, and J. Jones / Yaqalatqa7 (2024). "Líl̓wat oral traditions of Qwelqwelústen (Mount Meager): Indigenous records of volcanic eruption, outburst flood, and landscape change in southwest British Columbia". *Canadian Journal of Earth Sciences* 61(6), pages 661–677. DOI: 10.1139/cjes-2023-0098.

Wright, H. M., K. V. Cashman, E. H. Gottesfeld, and J. J. Roberts (2009). "Pore structure of volcanic clasts: Measurements of permeability and electrical conductivity". *Earth and Planetary Science Letters* 280(1–4), pages 93–104. DOI: 10.1016/j.epsl.2009.01.023.

Yonechi, F. (1988). "Aspect of the landscape of Bandai-san before the eruption". *Journal of Geography (Chigaku Zasshi)* 97(4), pages 317–325.

Zhang, K., X. Wu, R. Niu, K. Yang, and L. Zhao (2017). "The assessment of landslide susceptibility mapping using random forest and decision tree methods in the Three Gorges Reservoir area, China". *Environmental Earth Sciences* 76(11). DOI: 10.1007/s12665-017-6731-5.

Zou, H. and T. Hastie (2005). "Regularization and Variable Selection Via the Elastic Net". *Journal of the Royal Statistical Society Series B: Statistical Methodology* 67(2), pages 301–320. DOI: 10.1111/j.1467-9868.2005.00503.x.